Chapter IV

Studies on Microstructural Transition of Micellar Aggregates in Presence of Hydroxyaromatic Dopants: Rheology and Spectroscopy.

4.1. Introduction and Review of Previous Works

The self-assembly of amphiphilic molecules often develops a variety of interesting structures of different shapes and sizes. Among the most fascinating of these are the 'wormlike micelles', which are flexible cylindrical chains with radii of a few nanometers and contour lengths up to several micrometers. The formation of wormlike micelles is linked to the emergence of viscoelasticity in the solution [1,2]. Micellar aggregates that can grow anisotropically under appropriate conditions, changing their shapes from spheres to rods or highly flexible wormlike aggregates, provide some analogies between giant flexible cylindrical micelles and conventional polymeric solutions [3]. However, unlike ordinary polymers, micellar chains posess the unique ability to reversibly break and then recombine. They reform by addition and loss of individual amphiphiles or by the scission and recombination of entire micelles [1]. The polymerlike micelles which are formed by certain ionic surfactants in solution exhibit very interesting rheological properties. At high concentrations, these solutions show typical viscoelastic behaviour while at very low concentrations more complex and unusual rheological phenomena is observed. Wormlike micelles are formed spontaneously at ambient temperature from cationic surfactants with e.g. 16 carbon atoms in the aliphatic chain. This is the case for cetyltrimethylammonium bromide (CTAB) [4-6] and cetylpyridinium bromide (CPB) [7]. Because of electrostatics the transition between spherical to cylindrical aggregates occurs at relatively high surfactant concentrations. However, the growth of the aggregates can be promoted even at lower concentrations of the surfactant if cosurfactants or other low molecular weight additives are incorporated to the solutions. These additives are short alcohol

chains, strongly binding counterions, oppositely charged surfactants etc. Some of the different classes of surfactants and cosurfactants/additives which form such structures are given bellow.

A - Surfactant and simple salt. The addition of simple salts such as sodium chloride (NaCl) or potassium bromide (KBr) to ionic surfactant solutions results in the screening of the electrostatic interactions between the charges, and thus in the growth of the aggregates. Example of this class is CTAB with KBr [8-10]. Halide counterions bind moderately strongly to cationic surfactant aggregates, and therefore, micellar growth is gradual. Other well-known examples are sodium dodecyl sulfate (SDS) with monovalent [11, 12] or multivalent counterions [13,14]. Micellar geometry of the different microstructures formed by amphiphiles in solution can be understood on the basis of a term called the critical packing parameter or CPP, which is defined as as the ratio $v/a_o l_c$ (as has been discussed in chapter 1). The larger the headgroup area (a_o) compared to the tail area (l_c), the more curved the aggregate. Thus, a CPP of ⅓, corresponding to a cone shape, leads to spherical micelles while a CPP of ½ (truncated cone) corresponds to cylindrical micelles. Finally, molecules shaped like cylinders, i.e., having $a_o \approx l_c$ and CPP = 1, tend to assemble into bilayer structures (vesicles). When added to water, CTAB tends to form spherical micelles because the ionic headgroups have a large, effective area due to their electrostatic repulsions. However, when salt is added to CTAB, the added ions screen the repulsions between the cationic headgroups, reducing the headgroup area, and increasing the CPP from ⅓ to ½. As a result, CTAB forms cylindrical micelles that grow uniaxially into long chains.

B - Surfactant and cosurfactant, where the cosurfactant is a short alcohol chain. Classical examples are the ternary systems of sodium alkylsulfate-decanol- water (Sodiumdecylsulfate -Decanol [15,16], Sodiumdodecylsulfate-Decanol [17,18] and Cetylpyridinium Chloride-hexanol-brine (CPC-Hex) [19,20]. In these systems, the ratio between the alcohol and surfactant concentrations controls the polymorphism of the self-assembly. The theoretical arguments developed for neutral chains should apply to this class, namely those for which the cylindrical aggregates are intermediate structures between spheres and bilayers.

C – Surfactant and strongly binding counterion. Strongly binding counterions are small molecules of opposite charge with respect to that of the surfactant. They are also called hydrotopes. Well-known examples of hydrotopes are salicylate, tosilate and chlorobenzoate counterions, which all contain an aromatic phenyl group. CTAB and CPC with sodium salicylate (NaSal) have been probably the most studied micellar systems during the last two decades. Contrary to simple salts (class A), a large proportion of these counterions (~ 80 %) is assumed to be incorporated into the micelles. It was found that in CPC-NaSal, long wormlike micelles are immediately formed at the cmc (0.04 wt. %), without passing through an intermediate spherical morphology [21, 22].

D – Cationic and anionic mixtures. Oppositely charged surfactants have shown synergistic enhancements of rheological properties, and notably through the formation of mixed wormlike micelles. The growth of the micelles is assumed to arise from the charge neutralization of the surface potential (as in C) and from the related increase of the ionic strength (as in A). Recent examples are the mixtures of sodium dodecylsulfate (SDS) and dodecyltrimethylammonium bromide (DTAB) [23,24], or the mixtures made from cetyltrimethylammonium tosilate and sodium dodecyl benzenesulfonate [25,26].

That surfactant solutions can be strongly viscoelastic was noticed by several authors in as early as 1950's. Nash for instance identified the role of additives such as naphtalene derivatives in the onset of viscoelasticity in CTAB solutions [27]. One intriguing result was that the viscoelasticity of the solution was showing up well below the cmc of the surfactant. Some years later, Gravsholt and coworkers recognized that other types of additives, such as salicylate or chlorobenzoate counterions are actually solubilized by the micelles, lowering the c.m.c. of the surfactant [28,29]. It was suggested by the authors that the viscoelasticity had the same physical origin as that of polymer solutions [30]. The picture proposed in late 1970's was that of a network of entangled rod-like micelles.

A step further in the description of the micellar dynamics was made by the first quantitative measurements of the linear mechanical response, also known as Maxwellian Behaviour, of these solutions. The pioneering works in this field were

those of Rehage and Hoffmann [31-33], Shikata [34-37] and Candau [38,39] and their coworkers. Rehage and Hoffmann had used rheology to demonstrate that the micellar growth resulted in an increase of the fluid viscosity. They observed that the effect of addition of NaSal to CPC increased the viscosity of the system sharply until the concentration reached slightly above a 1:1 molar ratio of CPC/ NaSal and then the viscosity dropped off drastically. This feature was observed for several concentrations of CPC and there does not seem to have any satisfactory explanation of this phenomenon until this date. The most fascinating result that Rehage, Hoffmann, Shikata and Candau and their coworkers have observed by quantitative measurements was that the viscoelasticity of these surfactant solutions was characterized by a single exponential response function. This rule is indeed so general that it is now commonly admitted that a Maxwellian behavior is a strong indication of the wormlike character of self-assembled structures. In a detailed study of the tetradecyltrimethylammonium salicylate system, they also reported that an increase in flow birefringence accompanies the stress growth. Actually, both the stress and flow birefringence curves show an induction period before rapid growth commences. In addition to the general features as described, the induction time is shown to be inversely proportional to the applied shear rate and is independent of the flow direction. On the basis of this information, a kinetic coagulation mechanism, first introduced by Rehage, Wunderlich and Hoffmann [31] was proposed to account for the rheopectic phenomenon. According to this model, the initial small micelles collide with each other more frequently in shear flow than in quiescene, resulting in the formation of large micelles. The same results are also obtained when the influence of sodium salicylate and sodium bromide concentration on the shear thickening behaviour of aqueous micellar solutions of CTAB and NaSal is studied experimentally.

The effect of Sodium 3 hydroxy 2 naphtoate (3,2 SHCN) on the micellar shape transition of CTAB was investigated by Manohar and co workers [40-47]. The 3,2 SHNC which is structurally comparable to NaSal is strongly adsorbed on the micellar surface with the carboxylic and hydroxyl group protruding out of the micelle. The presence of naphthalene ring in HNC^- was expected to confer more hydrophobicity on the molecule as compared to NaSal. It was also proved from

surface tension measurements that SHCN is mildly surface active and considering the concentrations for such surface activity, it could be regarded as a hydrotope. The molecular orientation is consistent with the surface active nature of SHNC (compared to NaSal). However, the CTAB-SHNC system differs in a major way from CTAB-NaSal system through the presence of a sequence of phases viz., small micelle aggregates, an isotropic gel phase (non-birefringent rodlike micelle, L_1-Phase), anisotroic liquid crystal (birefringent Lamellar, L_α-Phase) -precipitate-liquid crystal etc. Recently Raghavan and co-workers have shown that when a mixture of a cationic surfactant with an erucyl (C_{22}, mono-unsaturated) tail and an organic salt, sodium hydroxynaphthalene carboxylate (SHNC) is heated their zero-shear viscosity, instead of dropping exponentially, increases over a range of temperatures [48]. Using small angle neutron scattering (SANS) technique, these authors, have shown that the increase in viscosity is caused by an increase in the contour length of cylindrical micelles.

It is particularly interesting that, while a wide variety of wormlike ionic micellar solutions display identical rheological responses, a common element in most of these systems is the presence of salt anions such as NaSal. Although a few examples are available in the literature where additives other than NaSal have been used as has already been mentioned, these molecules have never been considered as high up as the promoter like NaSal. The presence of an anionic charge on the promoter molecule has been considered pivotal in achieving low concentration shape transition of cationic micelles via charge screening because it decreases the average area per surfactant head group allowing the packing parameter to exceed the critical value of ⅓ [49]. However, other important factors including the role of OH group of the promoter molecule have not attracted much attention, and as such, the puzzling question as to why not only its presence but also its position in the aromatic ring of NaSal molecule is so vital remained broadly unanswered [50]. Therefore, to understand the role of the OH group precisely, it was tempting to check what would happen the uncharged naphthols, where the hydrophobic part is very strong and the anionic charge is absent, is used. In this chapter the effects of neutral 1- and 2-naphthols and also the dihydroxy derivatives, 2,3- dihydroxynaphthalene (2,3-DHN) and 2,7-

dihydroxynaphthalene (2,7-DHN), on the shape transition of CTAB micelles have been studied. The intermolecular H bonding between OH groups of micelle embedded naphthol molecules and the interfacial water molecules plays a key role in micellar shape transition in absence of any charge screening of head groups and thus imparts strong viscoelasticity to the dilute aqueous surfactant solution.

Since the effect of hydrogen bonding on the electronic spectra of organic molecules has been unambiguously detected and explained, the ultraviolet and visible spectroscopies are applied by a number of authors to study the hydrogen bond in solution. Investigation of the effect of hydrogen bonding on photodissociation of 1-naphthol was reported first by Takemura et. al. [51,52]. The ground state (UV-Vis absorption) and the excited state (fluorescence) solvatochromism of several naphthalene derivatives was analysed by Mataga and Kaifu [53] in terms of nonspecific solute-solvent interactions and specific hydrogen-bonding interactions. The influence of hydrogen bonding on the UV-Vis and emission spectra of naphthols has been studied by Baba and Suzuki [54] and Tramer and Zaborowska [55]. Switching of the lowest excited states of 1-naphthol, from ^1L_b state to ^1L_a state, as a result of better stabilisation due to hydrogen-bond interactions was suggested. While such studies on phenols and naphthols have been carried out in the presence of a variety of polar proton acceptor or donor solvent components in an inert solvent (or mixed solvents), similar investigations in organised media (micelles and vesicles) are scarce. Compared to a single solvent or a homogeneous mixture of solvents, organised assembly of nano dimensions possess many unique properties. The most significant property of an organised assembly is its ability to stabilise and bind solute molecules that are typically insoluble or sparingly soluble in bulk pure solvent [56]. Therefore, a detail investigation on the electronic spectra of indicator (probe) molecules in organised assemblies of CTAB, in particular and other alkyltrimethylammonium bromides in general, have been carried out to understand the mechanism of the phenomena of microstructural transitions in further detail.

The possibilities of the H bonding and π-π interaction in naphthols have been checked by observing the effect of CTAB micelles on the absorption spectrum of the hydroxyaromatic compounds. UV absorption spectra are modified due to

the presence of an intermolecular H-bond of micelle-embedded naphthols with the interfacial water in their ground electronic states. The excited state proton transfer (ESPT) of 2-naphthol is facilitated in the presence of CTAB in the submicellar concentration range due to the catalytic effect of surfactant charge, whereas ESPT is hindered in post-micellar concentrations due to lack of water accessibility [57]. However, the exact nature of H-bonding in the micellar phase is not understood completely. Moreover, together with hydrogen bonding, the π-π and cation-π interactions between favorably arranged micelle-embedded dopant molecules may also be involved in modifying the absorption spectra [58]. Therefore, in order to further examine the exact nature of the noncovalent interaction that is involved in the above modification of the spectra, it is tempting to check what would happen if the hydroxyl group of the promoter naphthol molecules is replaced by methoxy groups. Methoxynaphthalenes (MN) possess a similar structure and hydrophobicity to that of the hydroxyl naphthalene (HN) molecules but cannot act as hydrogen bond donors. It would be interesting to compare the efficiency of methoxynaphthalene with that of naphthols in effecting microstructural transitions of micelles and to discuss the result in the light of spectroscopic observations. Further, it may be anticipated that a simple and effective route to design a pH responsive microstructure could well be based on the neutral naphthol dopants, which form salts only at high pH (p*K*a > 9.2). As a function of pH, ionization of the OH group of naphthol molecules may switch the onset of charge screening, paving the way to effect further morphological transitions (viz., vesicle formation). An objective of the present work is, therefore, to design a simple effective route of pH-responsive morphological transition for the aqueous molecular aggregates of single chain cationic surfactant, viz., CTAB from micelles to long wormlike micelle to unilamelar vesicles. Finally, it is important to note that although the last two decades have witnessed a strong excitement among the researchers on the microstructural transitions of micelles at low concentrations, induced by hydrotropes like sodium salicylate and other similar dopants, leading to stimuli-responsive viscoelasticity, the exact role and the location of the protruded polar groups (e.g., OH groups) of the hydrotropes toward the Stern layer have not been firmly ascertained. This is particularly an interesting basic element to investigate for the present system where intermolecular H-bonding through OH groups of the

micelle-embedded naphthols seems to play the pivotal role in the transition of the micellar morphology.

The formation of wormlike micelles have been studied for various type of surfactants in recent years, and new applications have been found in different areas from oil fields, drag reducing agents in district heating systems, home and personal care products to templates for asymmetric and aligned nanostructures. Viscoelastic wormlike cationic surfactants have been successfully used as fracturing fluids in oil fields. Conventional polymer base fluid has comparable sand pack pore size residue left in reservoirs after fracturing. This reduces the fracturing permeability or conductivity. Surfactants, however, being small molecules, recovers back completely. Wormlike micelles are used commercially in district heating and cooling fluid as drag-reducing agents. The environmental friendly drag-reducing properties of N-alkyl, N, N-dimethylglycinate combined with sodium alkylbenzene sulfonate at a 4:1 molar ratio was found useful for such applications [59,60]. Viscoelastic property is needed in many home care products and microfluidity of wormlike micelle has such properties. A typical example of such application is hard surface cleaners and drain-opener liquid plumber, where the excellent thickening and cleaning capacity combined with easy flow and drag reduction properties have distinct advantages over other microscopic fluids such as lamellar or polymeric fluids. New applications should appear as our understanding increases and more and more application scientists understand the wormlike micelle system.

4.2. Materials and Methods

1- and 2-Naphthols (puriss, Aldrich) were purified by vacuum sublimation followed by crystallization from 1:1water methanol mixture. 1- and 2-Methoxynaphthalenes (Acros-Organics, Belgium) were recrystallized from 1:1 aqueous methanol before use. 2,3-dihydroxynaphthalene and 2,7-dihydroxynaphthalene were recrystalised twice from ethanol-water mixture and finally from ethanol alone. The structure of dopant molecules (probe) are shown in figure 4.1. All the probe molecules were stored in the dark. The surfactants viz.,

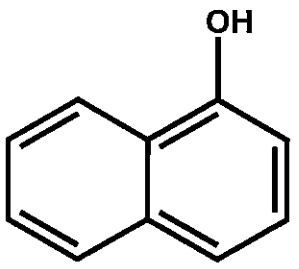

1-Naphthol

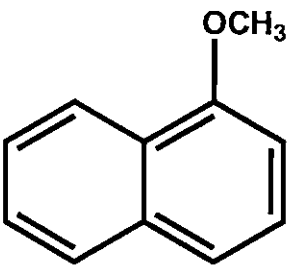

1-Methoxynaphthalene

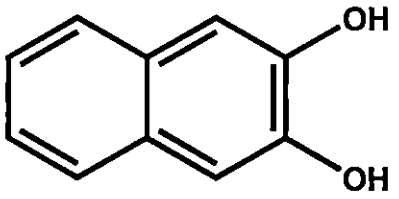

2,3-Dihydroxynaphthalene

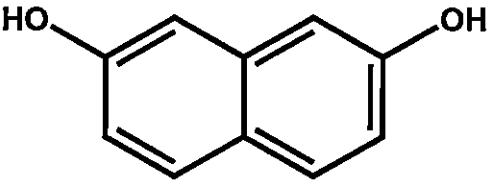

2,7-Dihydroxynaphthalene

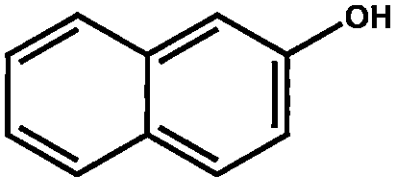

2-Naphthol

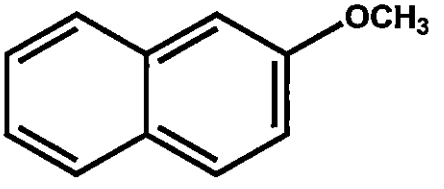

2-Methoxynaphthalene

Figure 4.1. Structures of the aromatichydroxy and methoxyaromatic dopants used in the present investigation.

Dodecyltrimethylammonium bromide (DTAB), Tetradecyltrimethylammonium bromide (TTAB), Cetyltrimethyl-ammonium bromide (CTAB) and Sodiumdodecyl sulphate (SDS) were of puriss grade procured from Aldrich and were used as received. Shear-induced viscosity was measured on a rotational viscometer (Anton-Paar, DV-3P; accuracy (1% and repeatability (0.2%)) equipped with a temperature controller and with the facility of varying shear rates. Here, the viscosity measurement is based on measuring the torque of spindle rotating at a given speed in the sample solution kept in a concentric cylinder, which is maintained at a constant temperature. The temperature of the viscometer was

regulated with a water circulating thermostat. The diameter and length of the inner cylinder are 2.5 cm and 9 cm respectively, whereas diameter and length of the outer cylinder are 2.8 cm and 14 cm respectively. The shear rate is calculated as rpm x 1.2236 s^{-1} (assuming the characteristics of the spindle). UV absorption spectra were recorded on a Jasco (V-530) Spectrophotometer using a matched pair of glass cuvettes. The instrument was attached with a water circulating thermostat. ^1H NMR spectra were recorded on a Bruker spectrometer (Germany) operating at 300 MHz. The water used for preparation of solutions was doubly distilled. The dopants (probes) were sparingly soluble in water at low pH but highly soluble in surfactants. Therefore, appropriate amount of the dopants were added directly to CTAB solutions. In some experiments dilute alcoholic solution of the dopants were used and alcohols were dried off before the addition of surfactant in the experimental set. Utmost care was taken to prepare naphthol-CTAB and other hydroxyaromatic dopant-CTAB solutions with minimum shaking. For the shear induced viscosity studies, the samples were equilibrated at desired temperatures in a thermostat (attached to the rotational viscometer) for 2 days before study.

4.3. Results and discussions

4.3.1. Shear Induced Viscosity Studies

Aqueous CTAB (2-10 mM) and 1- or 2-naphthol (2-10 mM in 2-5% methanol, naphthols being sparingly soluble in water) solutions show viscosities similar to those of water. But as soon as these solutions are mixed together at room temperature, a thick gel-type fluid with high viscoelasticity is developed. Since viscoelasticity tends to disappear in high methanol concentrations, experimental solutions are prepared routinely by transferring the required amount of naphthol solutions (in pure methanol) in the experiment vial first, and then the alcohol was evaporated off completely before the addition of aqueous surfactant solution. From the initial visual observation it was found that the viscosity of the gel was very much dependent on the concentration of CTAB and the additives. Therefore, we first determined the CTAB/dopant mole ratio at which the gel shows maximum viscosity. Much like the CTAB-NaSal system, it was found that CTAB-

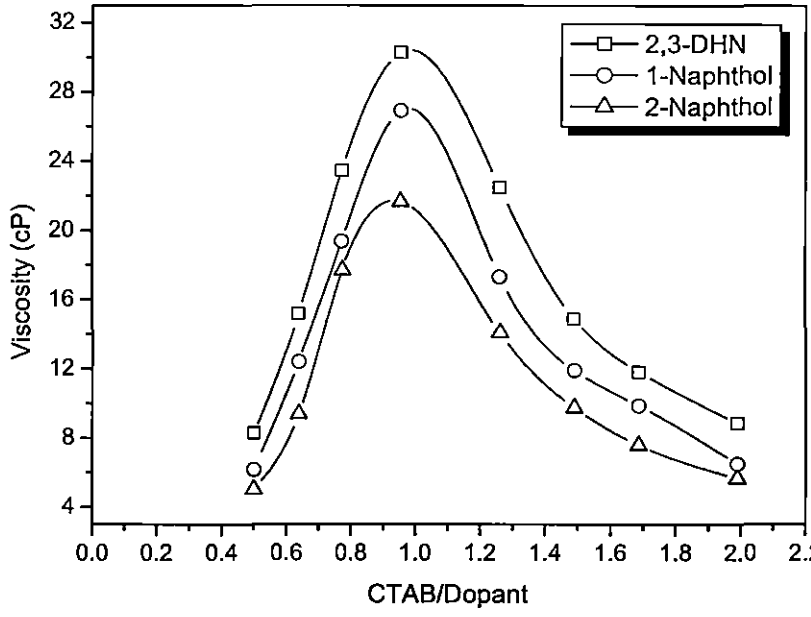

Figure 4. 2. Variation of viscosity as a function of mole ratio of CTAB and the dopants that form viscoelastic gels.

naphthols also display maximum viscoelasticity at a 1:1 molar ratio of surfactant and the promoter (figure 4.2). On the other hand, the effect of the dihydroxynaphthalenes (2,3-DHN and 2,7-DHN) on micelles of CTAB are interesting. Equimolar mixtures of only CTAB and 2,3-DHN gives a highly viscous gel in aqueous solutions but 2,7-DHN/CTAB does not. Therefore further attempts were not made to study the viscosity of 2,7-DHN/CTAB system. The argument that an excess or deficiency of charge on the micelles due to adsorption of hydrotrope anions (e.g., NaSal) would shorten the micellar life time and size is not apparently true for the present system because under the present experimental condition of solution pH (~6.5), the naphthols and the dihydroxynaphthalenes are mostly protonated, i.e., uncharged (p*Ka*'s > 9.0). Therefore, it seems apparent that the symmetrical distribution of surfactant and the promoter molecules, leading to highly compact spherical micelles, facilitates to attain an optimum surface curvature in presence of H bonding (discussed later), and this results in the sphere to rod transition easily. For further experiments, dopant to surfactant ratio was chosen to produce strongest viscoelasticity, i.e., 1:1 mole ratio. At low concentrations (<1 mM), CTAB-naphthol solutions show shear thinning properties, typically observed in the case of a non-Newtonian fluid. Typical plots

of viscosity against shear rate for 1- and 2-naphthols in CTAB solutions are shown in figures 4.3 and 4.4 respectively. Increasing the concentration range from 1 mM to 2 mM, the system shows a shear thinning property up to a shear rate of 25 s^{-1} and then the shear thickening phenomenon starts to occur, but above a shear rate of 60 s^{-1}, the fluid shows a Newtonian type behavior (figure 4.5 and 4.6). However, an overall non-Newtonian nature is apparent as the concentration of the CTAB and naphthol (1:1) system is raised above 1.0 mM. At still higher concentrations (>5.0 mM), the nature of the rheological response changes dramatically and the system starts displaying an unusual rheology as a function of shear rate. The variation of viscosity of CTAB/1-naphthol system as a function of shear rate at two different concentrations, 5.0 mM and 7.5 mM (1:1) is shown in figure 4.7. Up to a shear rate of 60 s^{-1}, the fluid shear thins. An onset of viscosity rise is observed at the shear rate of 60 s^{-1}, and the system again shear thins, passing through a maximum at 109 s^{-1}. At further higher concentrations (7.5 mM), the viscosity-shear rate profile again changes feature; the initial shear thinning characteristics disappear. The overall behaviour is consistent with building up of long worm-like micellar bundles at relatively high concentrations. Therefore, it appears that the shear thinning viscosity in low shear rates is indicative of the flow-induced alignment toward the flow directions. Equal concentrations of 2-naphthol/CTAB systems show similar features in the viscosity-shear rate profile (figure 4.8); the maximum viscoelasticity being displayed at 100 s^{-1}. Meanwhile, when the CTAB concentration is above 10.0 mM in the equimolar CTAB/naphthol solutions, the micelles are much longer and entangled with each other in the solution. In this case, the shear viscosity increases much higher and the micellar solution behaves like entangled polymer solutions exhibiting typical nonlinear viscoelastic behavior such as a stress plateau. The contour length of the worm-like micelles is highly dependent on the concentrations of the surfactant and the promoter. The viscosity shear rate profile for the 2,3-DHN/CTAB systems are shown in figures 4.9 to 4.11. The rheological characteristics shown by this system is almost similar to those of the CTAB-naphthol systems. Systems which display shear induced nonlinear rheological changes (as the present systems) bring about formidable problem in measuring the unperturbed solution viscosity because, the measuring techniques

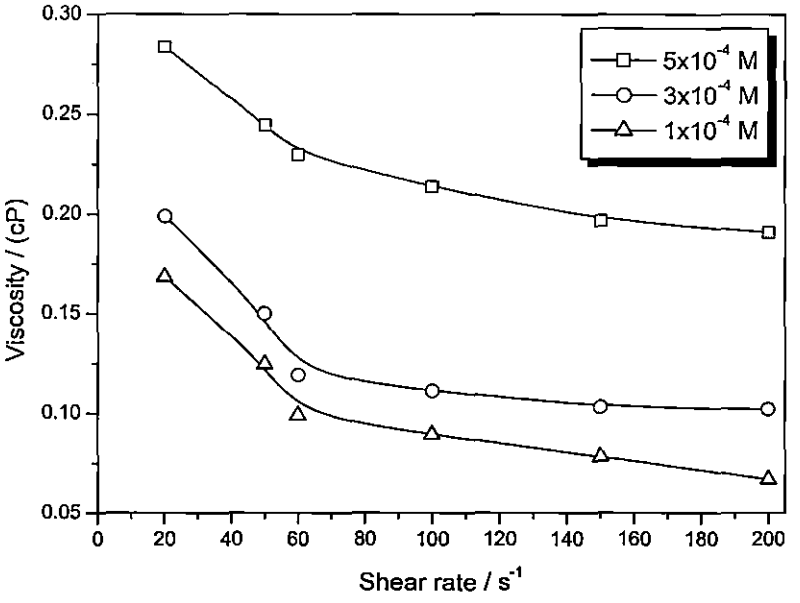

Figure 4.3. Variation of viscosity of 1-naphthol/CTAB system as a function of shear rate at different molar ratios.

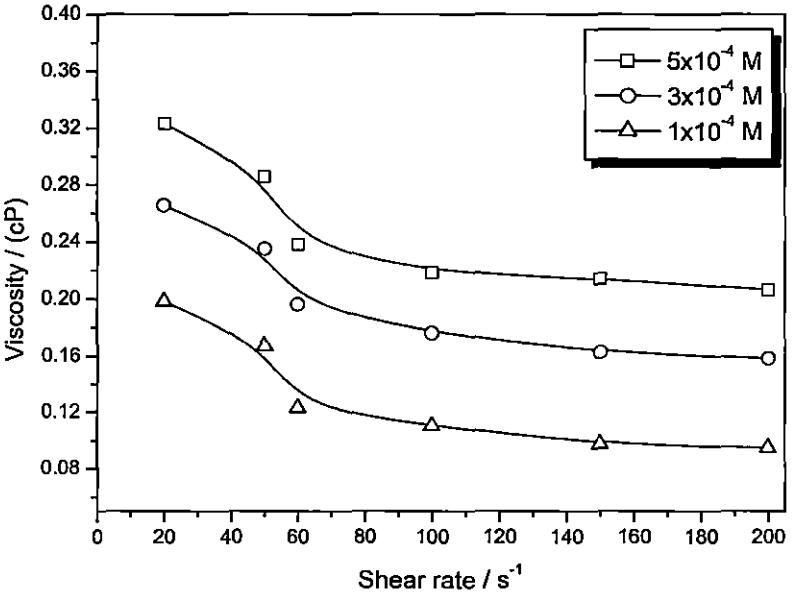

Figure 4.4. Variation of viscosity of 2-naphthol/CTAB system as a function of shear rate at different molar ratios.

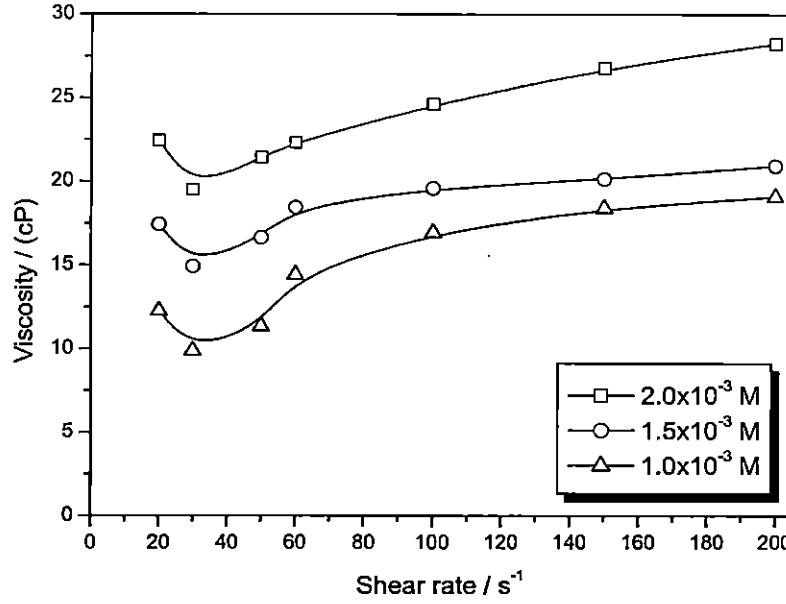

Figure 4.5. Variation of viscosity of 1-naphthol/CTAB system as a function of shear rate at different molar ratios.

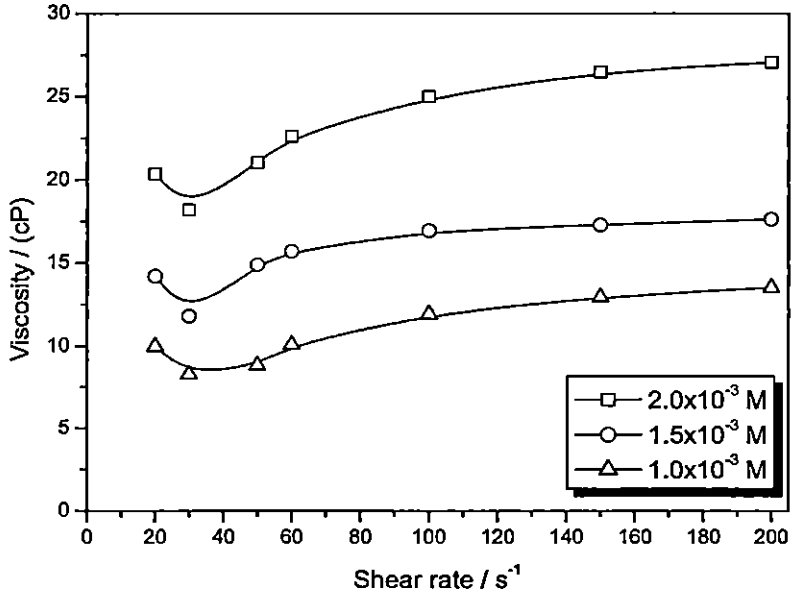

Figure 4.6. Variation of viscosity of 2-naphthol/CTAB system as a function of shear rate at different molar ratios.

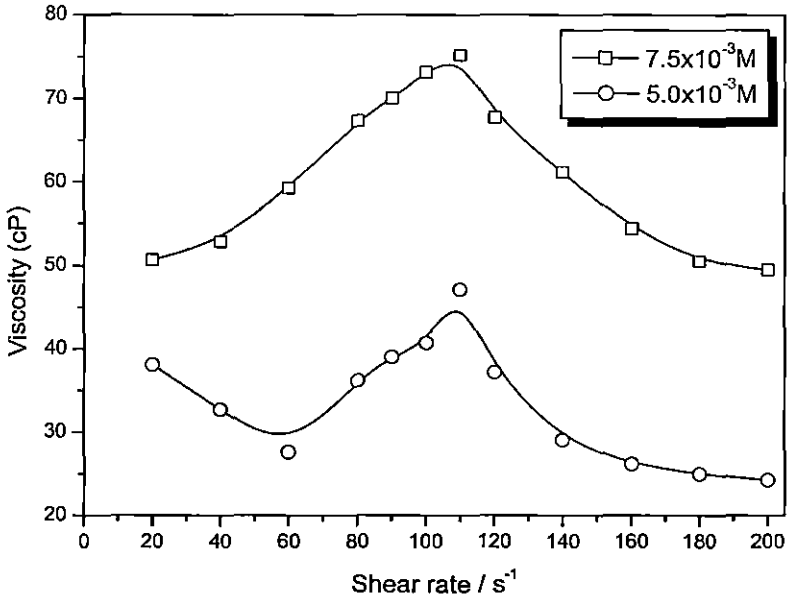

Figure 4.7. Variation of viscosity of 1-naphthol/CTAB system as a function of shear rate at different molar ratios.

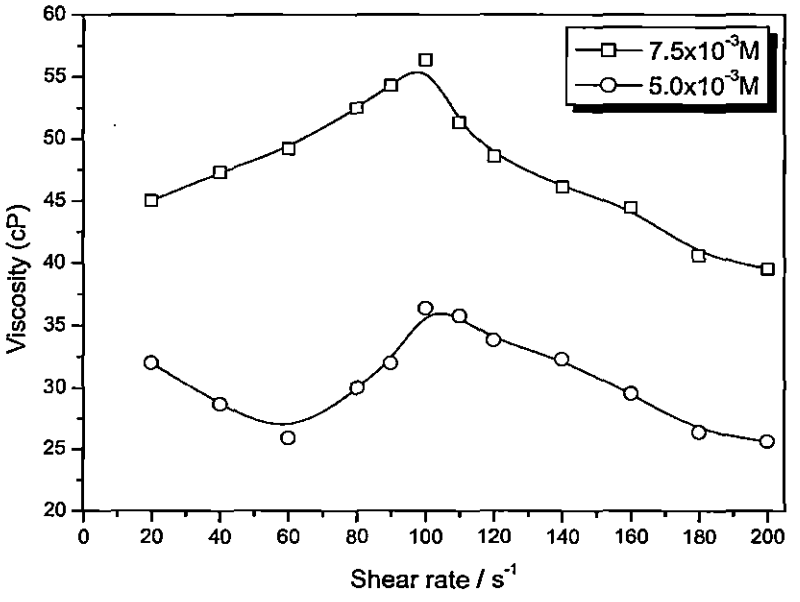

Figure 4.8. Variation of viscosity of 2-naphthol/CTAB system as a function of shear rate at different molar ratios.

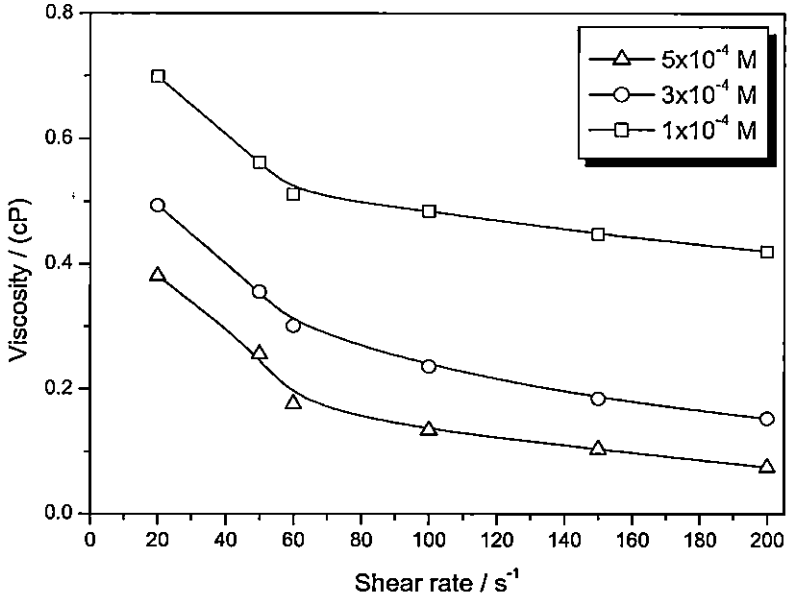

Figure 4.9. Variation of viscosity of 2,3-dihydroxynaphthalene/CTAB system as a function of shear rate at different molar ratios.

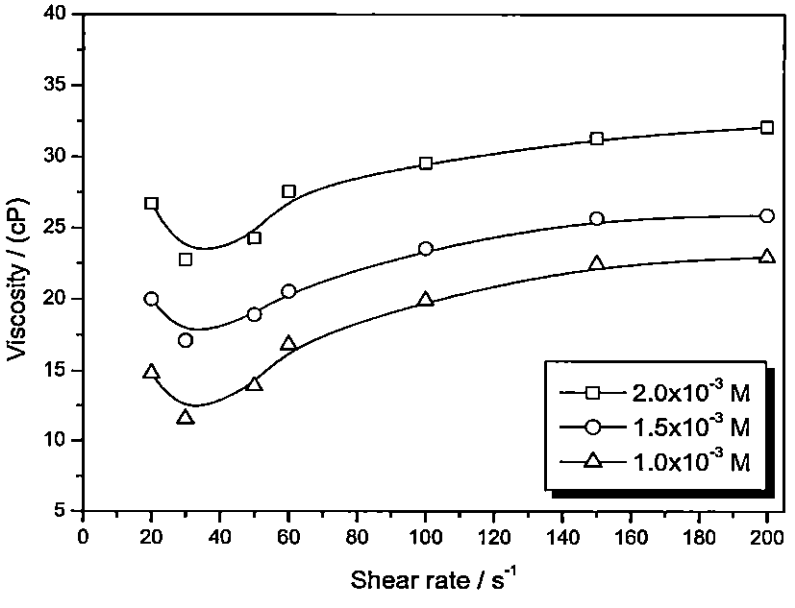

Figure 4.10. Variation of viscosity of 2,3-dihydroxynaphthalene/CTAB system as a function of shear rate at different molar ratios.

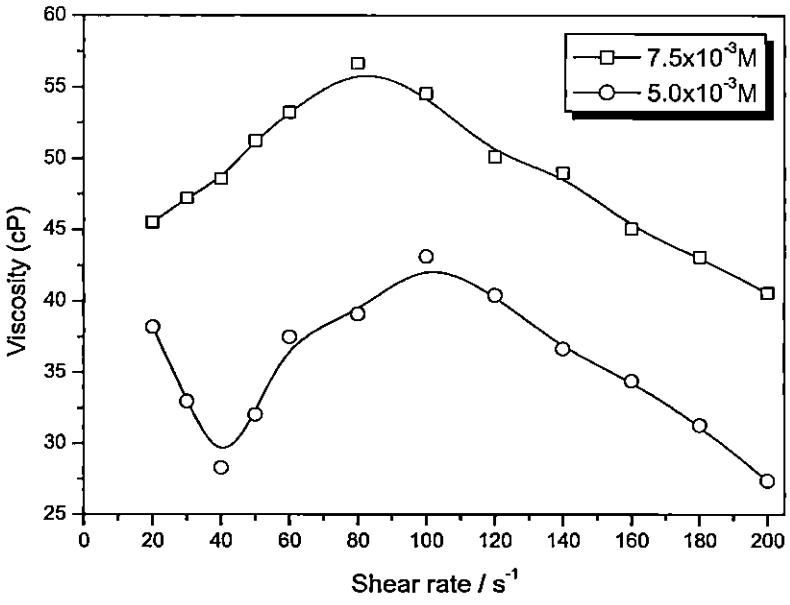

Figure 4.11. Variation of viscosity of 2,3-dihydroxynaphthalene/CTAB system as a function of shear rate at different molar ratios.

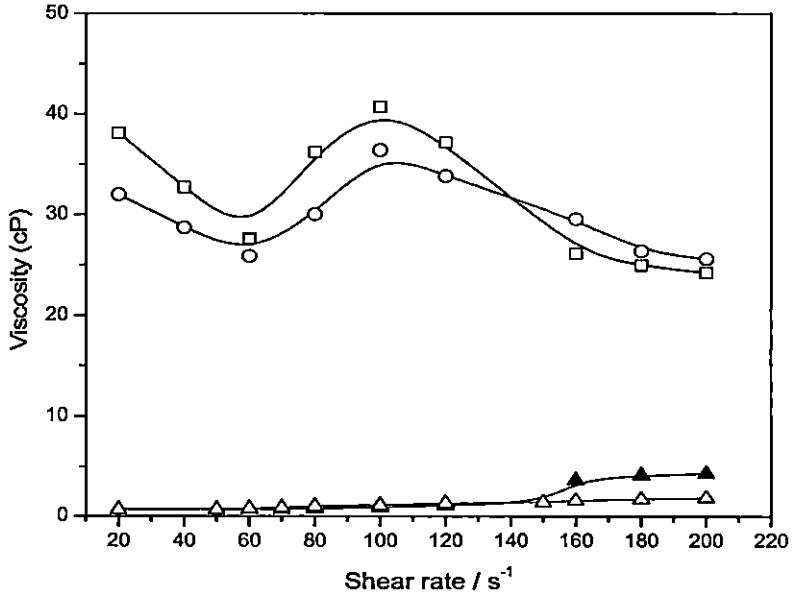

Figure 4.12. Comparision of viscosity modification of aqueous CTAB by 1-methoxy-naphthalene ( ), 2- methoxynaphthalene (▲), 1-naphthol (□) and 2-naphthol (O) at 25°C. The concentration of the dopant and the surfactant was fixed at 5 mM (1:1).

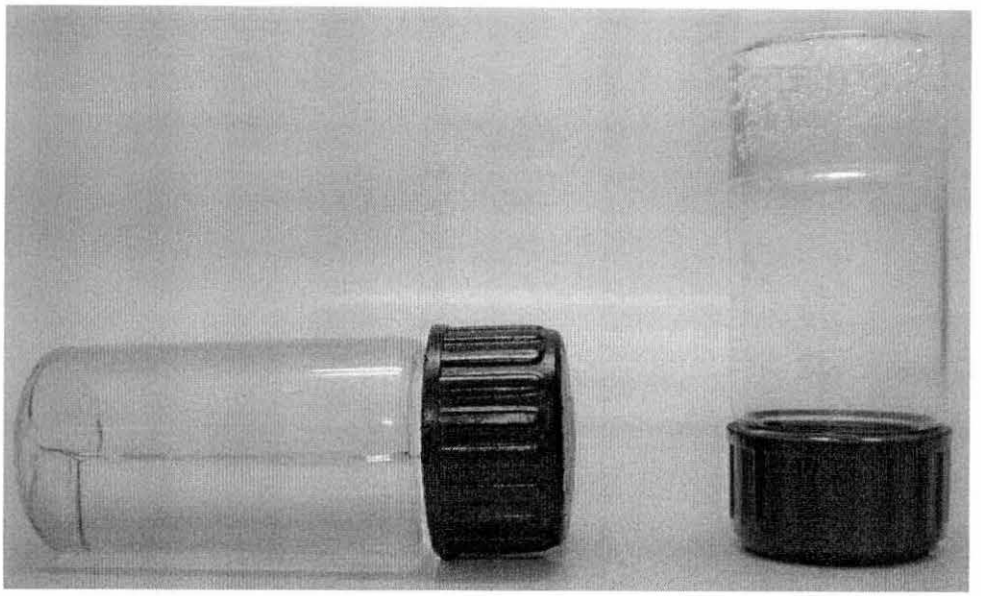

Figure 4.13. Photographs of the viscoelastic-gel (right) of aqueous 1-naphthol/CTAB (0.1 M, 1:1) and free flowing 'water like' solution (left) of 1-methoxy-naphthalene/CTAB system (0.1 M, 1:1).

(e.g., torsional shear rheometry) often apply considerable stress on the system during measurement, and thus the zero-shear viscosity becomes obscure.

The methoxynaphthalene-CTAB systems (1-methoxynaphthalene/CTAB and 2-methoxynaphthalene/CTAB), on the other hand, neither display the ability to develop viscoelasticity in the system nor exhibit any viscosity modification with applied shear, and behave completely like a Newtonian liquid. This result is quite surprising in view of the fact that much like 1- and 2-naphthols, both 1- and 2-methoxynaphthalenes are expected to embed into the micelles of CTAB. The plot of viscosity against shear rate for both the methoxynaphthalenes are shown in figure 4.12. For comparision the values of the naphthols at similar concentrations and conditions are also included in the figure. The images of the naphthol/CTAB and methoxynaphthalene/CTAB systems at 25°C are shown in figure 4.13. Though methoxynaphthalenes (MN) possess similar structure and hydrophobicity to that of the hydroxynaphthalene (HN) molecules but because the methoxynaphthalenes cannot act as hydrogen bond donors, they fail to assist the micellar shape transition and can not impart viscoelasticity to the CTAB solution. The exact role of

hydrogen bonding in micellar shape transition has been discussed later in the light of spectroscopic observations.

4.3.2 Effect of Temperature.

Typically, when a wormlike micellar solution is heated, the micellar contour length decays exponentially with temperature. At higher temperatures, surfactant unimers can move more rapidly between the cylindrical body and hemispherical end cap of the worm (the end cap is energetically unfavorable over the body by a factor equal to the end-cap energy). Thus, because end-cap constraint is less severe at higher temperatures, the worms grow to a lesser extent. However, an opposite trend in the rheological behavior is observed in CTAB-naphthol systems. Plots of viscosity against temperature, at shear rates of 35, 70, 120 and 200 s^{-1} for 1-naphthol, 2-naphthol and 2,3-dihydroxynaphthalene in presence of CTAB solutions are shown in figures 4.14-4.16. Instead of a decrease in viscosity, it is increased with temperature steadily up to a critical temperature value (26°C for CTAB-naphthols) and then decreases. This transition as a function of temperature is reversible, i.e., if the temperature is lowered down from a high value, viscosity of the system follows the same viscosity-temperature profile. This observation is unusual, and the only example of this kind is found in a recent reference where wormlike micelle formation was promoted by sodium salt of hydroxynaphthalene carboxylate (SHNC) [48]. The micellar growth in the above systems is attributed to a desorption of weakly bound HNC counterions from the micelle at elevated temperatures. Such a desorption is believed to reduce the charge density at the micellar interface and thereby promote the growth of cylindrical structures. However, any explanation emphasizing charge screening of surfactant head groups by the added salt anions as has been put forward in above experiments is not applicable to the present system. On the other hand, hydrophobic interaction between micellar core and the aromatic ring of the dopant molecules seems to be an important factor, which imparts the thermoreversible viscoelastic property to the present system. As temperature is increased, naphthol molecules (uncharged) are more soluble and perhaps are partitioned more strongly in the micellar phase.

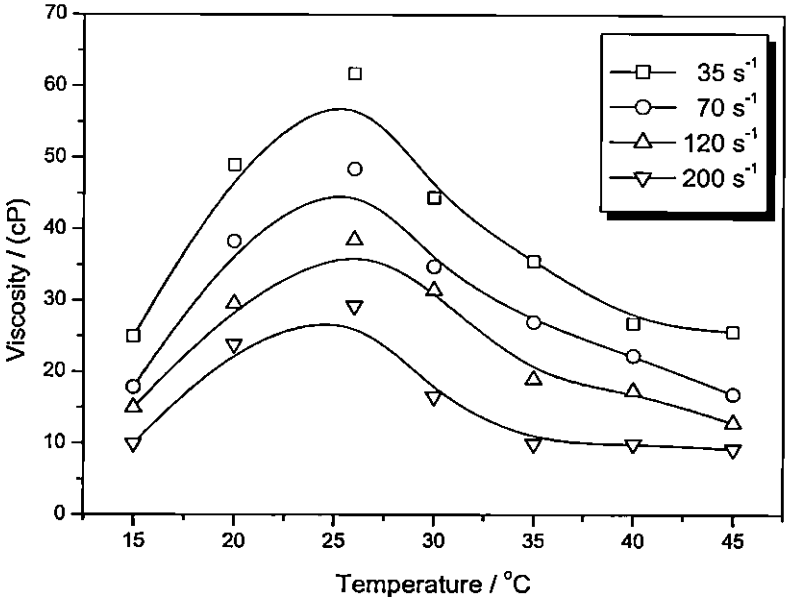

Figure 4.14. Variation of viscosity of 1-naphthol/CTAB system (10 mM; 1:1) with temperature at different shear rates.

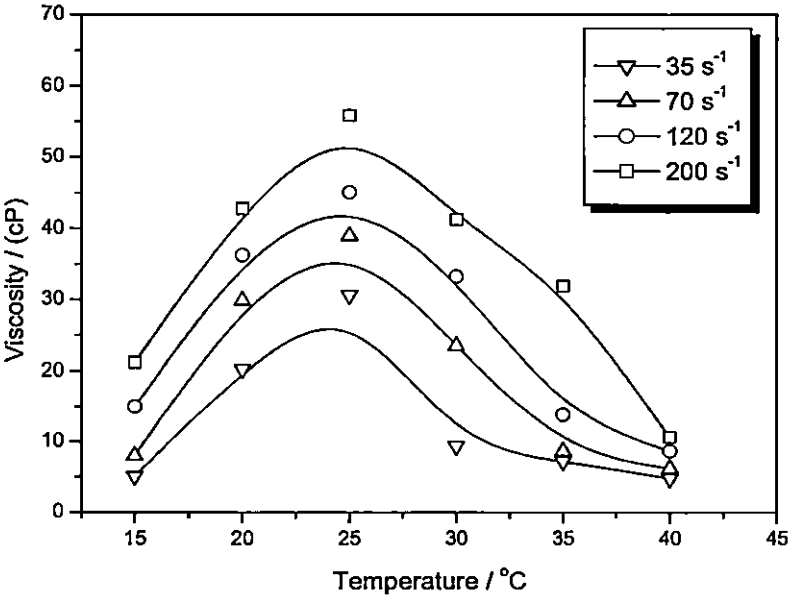

Figure 4.15. Variation of viscosity of 2-naphthol/CTAB system (10 mM; 1:1) with temperature at different shear rates.

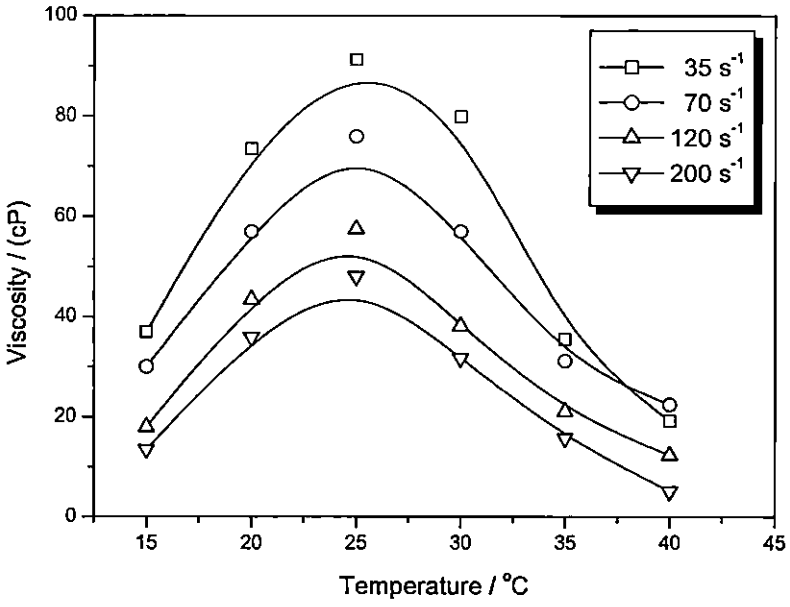

Figure 4.16. Variation of viscosity of 2,3-dihydroxynaphthalene/CTAB system (10 mM; 1:1) with temperature at different shear rates.

This favors the formation of longer wormlike micelles up to the critical temperature, above which the increased kinetic energy allowing surfactant unimers to hop more frequently between the body and the end cap results in the breaking up of the wormlike micelles [48].

4.3.3. Shear-Induced Viscosity and pH.

The role of neutral hydroxyaromatic dopants, viz., 1- and 2-naphthols, which are found to be efficient in bringing about microstructural transition in CTAB micelles, stimulates the idea of designing a route for pH-responsive vesicle formation [57]. This idea stems from the fact that the dopants, which under neutral conditions activate the formation of worm-like micelles at pH ~5.0, may on partial ionization of the OH group increase the packing parameter further via charge screening [61]. This idea tempted the investigator to study the pH dependent viscosity changes of the present viscoelastic gel system. Figures 4.17 and 4.18 shows the viscosity-pH profiles of the 1-naphthol-CTAB and 2-naphthol-CTAB systems at constant shear of 122 and 184 s^{-1}, respectively. The general nature of the variation of viscosity as a

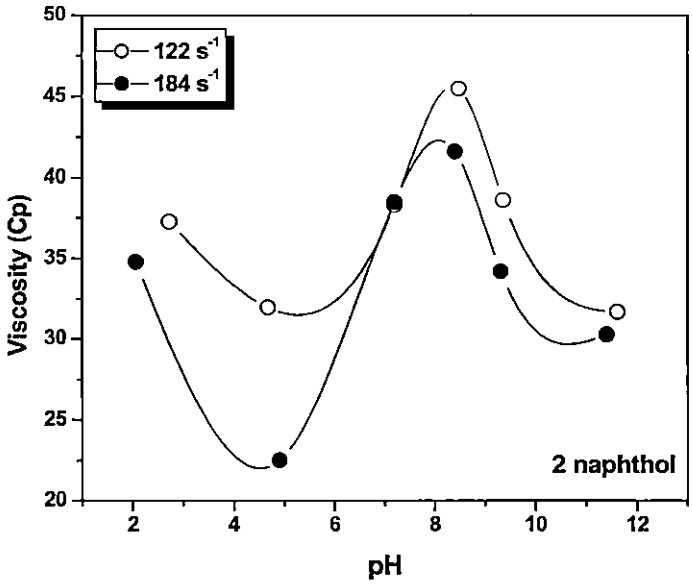

Figure 4.17. Viscosity vs pH profile for 2-naphthol/CTAB systems at fixed shear rates of 122 and 184 s^{-1}.

function of pH for both 1- and 2-naphthol-CTAB systems is similar in high shear regime (viz., 122 and 184 s^{-1}, respectively). However, morphological responses are not identical for both of the systems. While the viscosity of both, 2- as well as 1-naphthol-CTAB systems, is quite high (35-45 cP) due to formation of long worm-like micelles at low pH, the viscosity of the former system falls initially, indicating formation of shorter micelles until pH ~5.0 is reached. Charge screening by the anions from the added acid may be responsible for this observation. On the other hand, for 1-naphthol-CTAB, the onset of viscosity rise as a function of pH is found to occur from very low pH (pH ~2.0). For 2-naphthol-CTAB, the onset of viscosity rise is observed at higher pH (>5.0) and the viscosity-pH profile passes through a maximum at pH ~8.5. The onset of viscosity rise is observed due to the partial titration of OH group, leading to charge screening of surfactant head groups by the naphtholate anion and at pH ~8.5 the worm-like micelles grow maximum. Additional increase in pH results in the ionization of OH group further, and the packing parameter probably exceeds the critical value of 1/2 via enhanced charge screening, leading to vesicle formation (for naphthols, p*Ka* > 9, which means 50% ionization of the OH group at pH ~9.0). This results in the fall of viscosity of the system. Since 1-naphthol could modulate the micellar surface curvature of CTAB

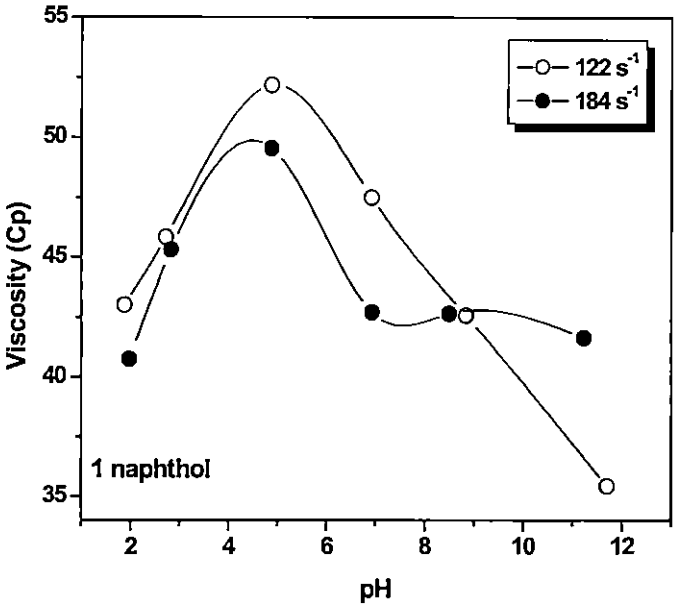

Figure 4.18. Viscosity vs pH profile for 1-naphthol/CTAB systems at fixed shear rates of 122 and 184 s^{-1}.

more efficiently, a little dissociation of the OH group (at low pH range) leads to an appreciable decrease of surface curvature via charge screening and promotes long worm-like micelle formation. In fact, for the 1-naphthol-CTAB system, vesicles start to form even at slightly higher than pH ~5.0 (Figure 4.18). A simple and effective route to design pH responsive viscoelastic worm-like micelles and less viscous globular vesicles based on naphthol dopants may be tuned by controlling the degree of charge screening of CTAB micelles via controlled ionization of naphtholic OH groups. The result of pH-responsive morphology modification is further investigated by means of cryo-TEM (discussed later).

4.3.4. Spectroscopic studies

4.3.4.1 ^{1}H NMR study.

To ascertain the location and orientation of the additive naphthol molecules in the micelles and to understand the nature of interaction in micellar shape transitions, ^{1}H NMR experiments may be helpful along with the absorption spectroscopies. NMR spectrum of 2-naphthol in D_2O (in absence of CTAB) shows clusters of

signals centered at δ values of 7.850 and 7.382, respectively, due to the resonance of the aromatic ring protons (figure 4.19 a). These two sets of signals are shifted upfield, broadened, and merged to give two broad signals at δ values of 7.337 and 6.991, respectively, when D_2O solution of CTAB and naphthols are mixed in 1:1 molar ratio (1.0 mM; Figure 4.19 b). This large shift of aromatic proton resonance to low δ values clearly indicates the location of naphthol rings in the less polar environment than that of water. Previous studies with CTAB-NaSal system also showed similar upfield shift of proton resonance of the aromatic moiety of NaSal molecule, and it was argued that this was due to insertion of Na Sal molecules into the micelles [50]. On the other hand, CH_3 protons of CTAB head group and the adjacent CH_2 protons, which resonate at 3.132 and 3.289, respectively, in D_2O (Figure 4.19 c), are shifted upfield and resonate at 2.746 and 2.397, respectively, in the presence of 2-naphthol (Figure 4.19 d). However, CH_2 protons adjacent to CTAB head group, are affected most in the presence of naphthols, and unlike pure CTAB, the signal from CH_2 protons emerges on the other side of CH_3 protons of CTAB head groups in the presence of naphthols. This identification is important because it indicates the presence of aromatic ring of naphthol near the surfactant head groups and close to adjacent CH_2 group. Signals from protons of other parts of hydrocarbon chain, however, remain unaffected in presence of naphthols (Figure 4.19 e). The NMR spectra of 10 mM CTAB-2-naphthol (1:1) have further subtle features (Figure 4.20). While the signals from water protons remain well resolved (not shown), the signals from the aromatic protons of the naphthol molecules are broadened dramatically (Figure 4.20 a). This means that on the NMR time scale, the motion of the naphthol molecules is highly restricted in viscoelastic phase, but water molecules rotate freely [62]. The signals from CTAB protons are, however, broadened to a lesser extent but appear structureless preventing further analysis (parts b and c of Figure 4.20). It seems that the naphthol molecules are held tightly in the micelles by means of strong hydrophobic interaction and H bonding (discussed later). Above observation conclusively proves that the solubilized naphthol molecules are penetrated not deep inside the micellar core but present near the surface probably with a well-defined orientation in which the OH groups are protruded from the micellar surface toward the polar aqueous phase.

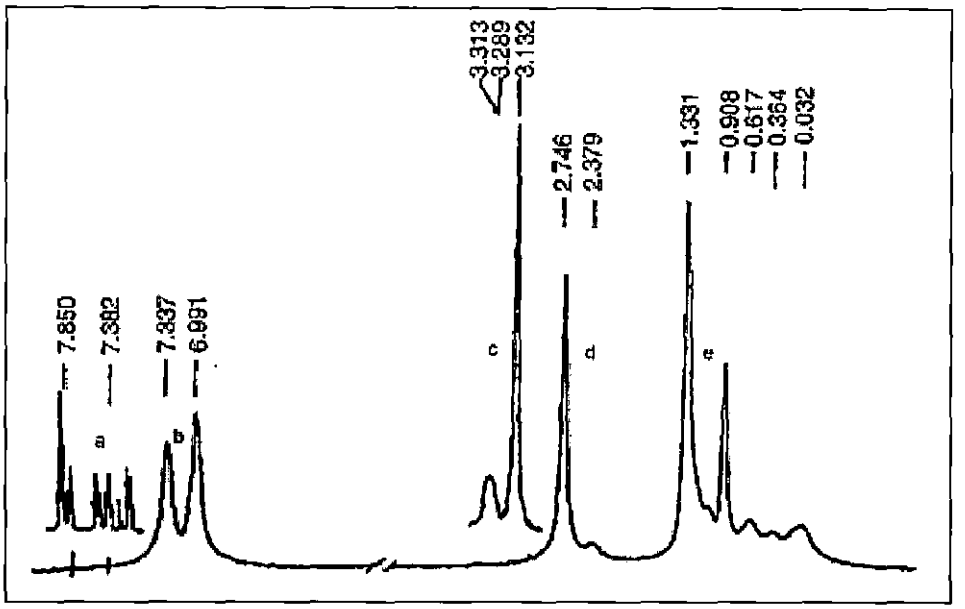

Figure 4.19. ^{1}H NMR spectra of CTAB-2-naphthol system. (a) ^{1}H signal from 2-naphthol, (c) ^{1}H signal from CTAB, (b, d, e) NMR spectrum of CTAB-2-naphthol (1 mM, 1:1).

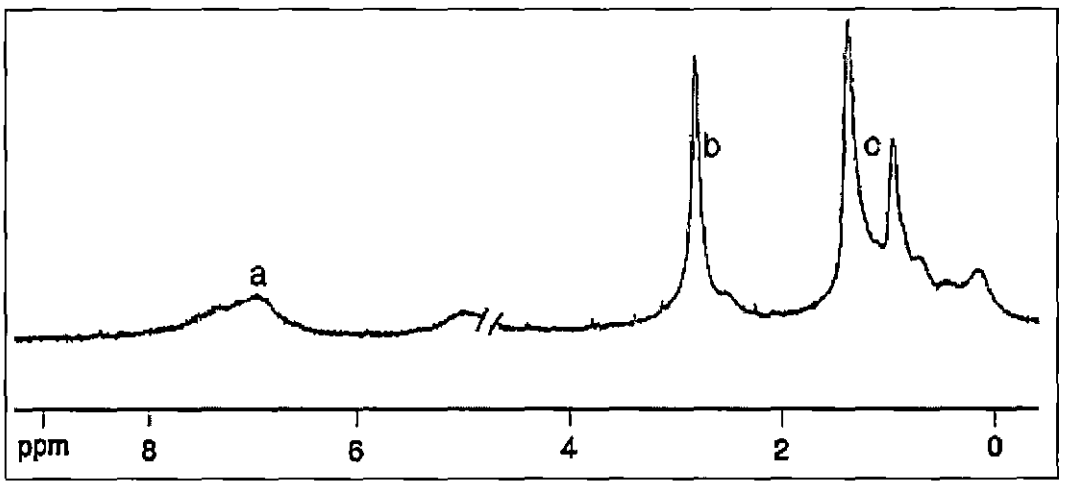

Figure 4.20. ^{1}H NMR spectra of CTAB–2--Naphthol system; abc: NMR spectrum of CTAB–2–Naphthol (10.0 mM, 1:1).

A previous study on the measurement of "apparent" shift of p*Ka* of 1-naphthol at the micellar surface of CTAB yielded an effective dielectric constant value of ~45, indicating that the location of OH groups of naphthol at the micellar surface is fairly polar in nature [63, 64].

The orientation of 2,3-DHN and 2,7-DHN molecules within the micelle is greatly determined by the position of the substituents (-OH) on the aromatic ring. Though H-bonding between the water molecules and the micelle embedded dihydroxynaphthalenes is possible for both 2,3-DHN and 2,7-DHN, it is to be noted that equimolar mixtures of only CTAB and 2,3-DHN gives a transparent and highly viscous gel in aqueous solutions but 2,7-DHN/CTAB does not. Therefore, to ascertain the location and orientation of 2,3-DHN and 2,7-DHN molecules in the micelles and to understand the nature of interaction in micellar shape transitions, ^{1}H NMR studies of both the probes in CTAB micelles were also carried out in D_2O. NMR spectrum of 2,3-DHN in D_2O (in absence of CTAB) shows three sets of signals centered at δ values of 7.236, 7.283 and 7.652 respectively, due to the resonance of the aromatic ring protons (Figure 4.21). All the three sets of signals are shifted upfield, broadened, and merged to give broad signals at δ values of 6.732, 6.895 and 7.143, respectively, when D_2O solution of CTAB and 2,3-DHN are mixed in 1:1 molar ratio (3.0 mM;). The large shift of aromatic proton resonance to low δ values indicates the location of naphthalene rings in the less polar environment than that of water. The broadening of aromatic proton signals is typical for a wormlike micellar solutions. The NMR spectrum of 2,7-DHN, on the other hand, in D_2O (in the absence of CTAB) shows three sets of signals at *δ* values of 6.932, 7.051 and 7.712, respectively, due to the resonance of the aromatic ring protons (Figure 4.22). These three sets of signals are shifted slightly upfield and resonate at δ values of 6.753, 6.782 and 7.401, respectively, when D_2O solution of CTAB and 2,7-DHN are mixed in 1:1 molar ratio (1.0 mM). Unlike the 2,3-DHN/CTAB system, the signals are not broadened and remain well resolved. The upfield shift of proton resonance for the 2,7-DHN in CTAB micelles is small compared to that of 2,3-DHN. This shows that in micellar solutions of CTAB, the 2,7-DHN molecules are portioned in somewhat less polar environment than that of water, but resides in a far more polar surroundings than that of 2,3-DHN molecule

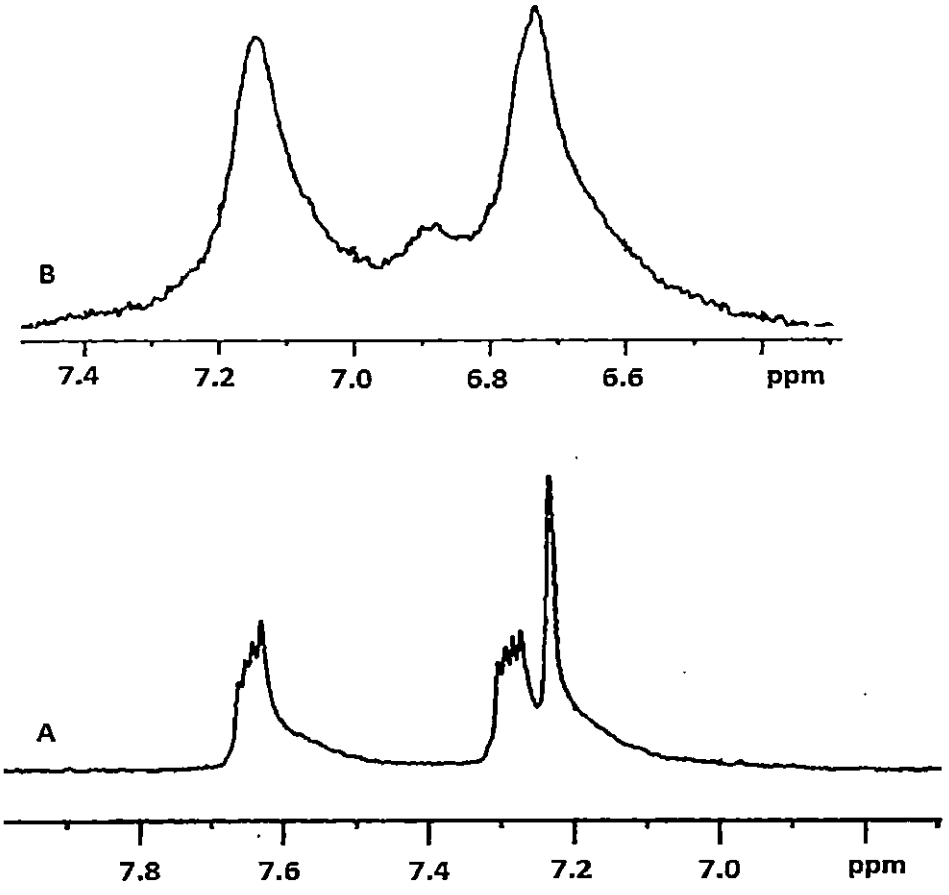

Figure 4.21 . ^{1}H NMR spectra of 2,3-dihydroxynaphthalene in the absence (A) and presence (B) of CTAB (7.5 mM, 1:1).

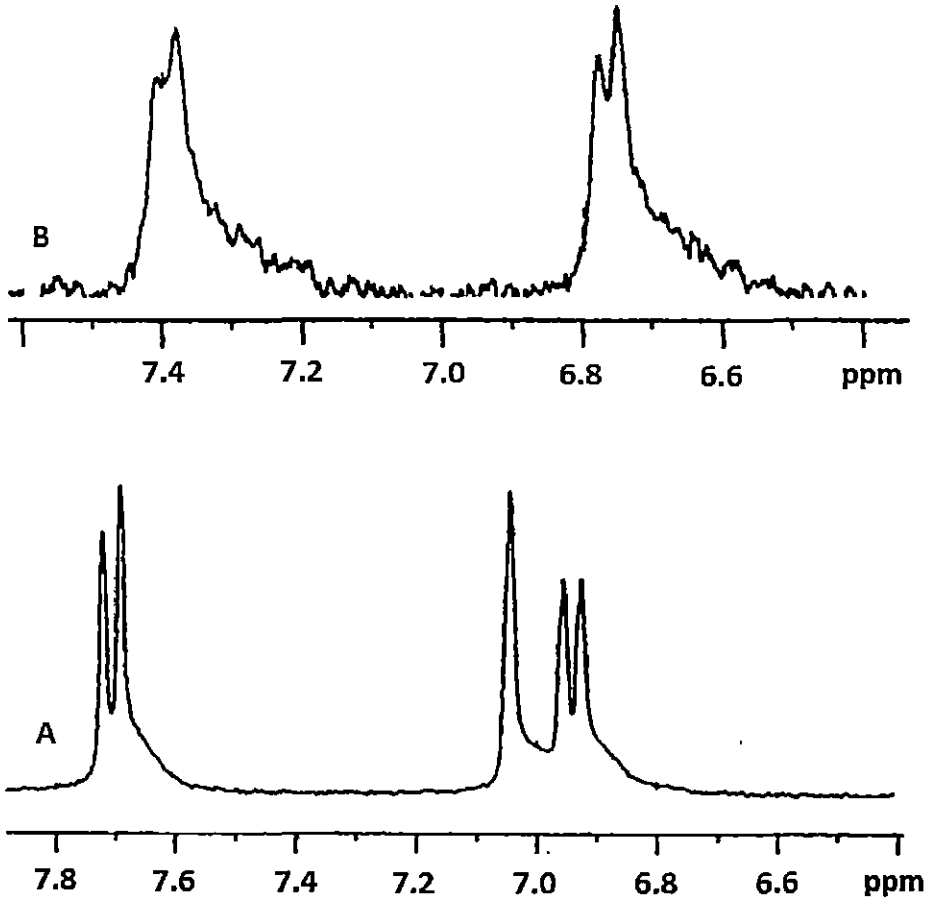

Figure 4.22 . ^{1}H NMR spectra of 2,7-dihydroxynaphthalene in the absence (A) and presence (B) of CTAB (7.5 mM, 1:1).

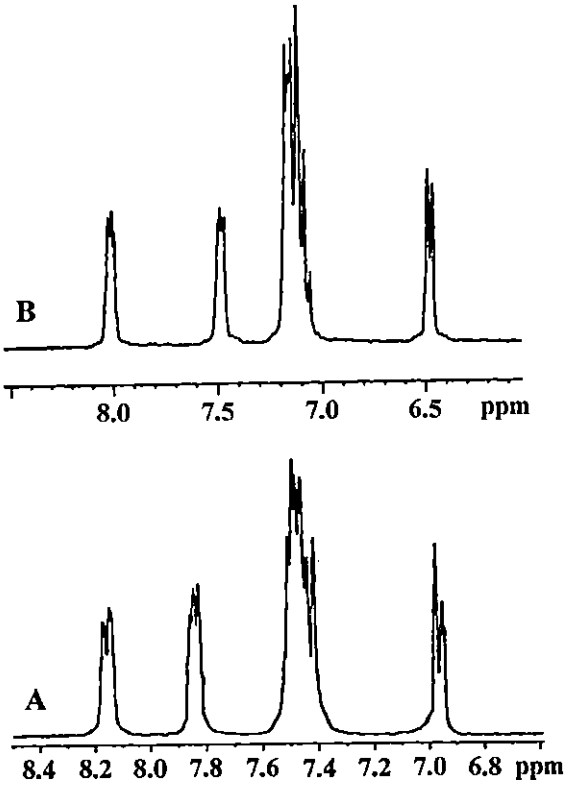

Figure 4.23. ^{1}H NMR spectra of 1-methoxynaphthalene in the absence (A) and presence (B) of CTAB (7.5 mM, 1:1).

Also, the absence of line broadening and presence of well resolved structures of the NMR signals clearly indicates fast rotation of naphthalene rings in the CTAB-2,7-DHN systems. To understand the nature of interaction of the additive methoxynaphthalene (1 MN and 2 MN) molecules with the CTAB micelles, ^{1}HNMR experiments were also performed (figure 4.23). NMR spectrum of 1MN in D_2O (in absence of CTAB) show signals centered at δ values of 8.151, 7.853, 7.482, and 6.947 respectively, due to the resonance of the aromatic ring protons (figure 4.23 A). All the four sets of signal are shifted upfield, remain well resolved and appear at δ values of 8.013, 7.492, 7.147 and 6.487 respectively, when D_2O solution of CTAB and 1 MN are mixed in 1:1 molar ratio (7.5 mM; Figure 4.23 B). Similarly, the methoxy protons which resonate at a δ value of 3.953 in water (not shown) are also shifted up-field and resonate at a δ value of 3.561 in CTAB. This large shift of aromatic proton resonance as well as the methoxy proton signals to low δ values again indicates the location of naphthalene rings and methoxy protons in the less polar environment than that of water. Unlike naphthol-CTAB systems, absence of

line broadening and the well resolved structures of the NMR signals clearly indicates fast rotation of naphthalene rings in the CTAB-MN systems (on NMR time scale). However, the degree of upfeild shift of the signals is less in 1 MN than that in naphthols; this indicates a stronger partitioning of naphthol molecules in the micelles than those of methoxynaphthalene (figure 4.23).

4.3.4.2. UV-Visible spectroscopy

Spectral Modification of Micelle-Embedded Dopants: Contribution of H-Bonding, π-π or Cation-π Interactions?

In view of the differences in the viscoelastic responses and the morphological transitions of CTAB micelles (Figure 4.12) induced by neutral naphthols and the methoxynaphthalenes, UV absorption spectra of these dopants may be interesting to study in micellar media. To understand the kind of interactions which are operative in the micelle-dopant systems, the key element of the present study is to compare the spectral characteristics of naphthols (which contain OH) with those of methoxynaphthalene (which do not contain OH) under various conditions in order to visualize a consistent molecular picture eliminating the untenable suggestions. Aromatic compounds, e.g., naphthalene, in general, have two strongly overlapped bands in the near UV region, viz., the longitudinally polarized $^1L_a \leftarrow {}^1A$ band and the transversely polarized $^1L_b \leftarrow {}^1A$ band. While the vibrational structure of these bands appears differently in different substituted compounds, effects of extending conjugation in 1 and 2 positions by OH or CH_3O groups in naphthol and methoxynaphthalene molecules, respectively, are interesting. Both in 1-naphthol and 1-methoxynaphthalene conjugation is extended in the transverse direction and, therefore, it affects the transverse polarized ^1L_a band. In 2-naphthol and 2-methoxynaphthalene, on the other hand, conjugation is primarily extended in the longitudinal direction, affecting both the intensity and the frequency of the longitudinally polarized ^1L_b band compared to the unsubstituted naphthalene.

It is well-known that the near UV spectra of aromatic compounds are affected by specific interactions like hydrogen bonding. Noncovalent interactions

like π-π and cation-π also cause shifts in the electron distributions of the molecule. The OH group of naphthols can act as both a proton donor as well as a proton acceptor in forming intermolecular hydrogen bonding. A hydrogen bond in which the hydroxyl groups of naphthols is a proton donor releases electron density from the O-H bond toward the oxygen and hence, by an inductive effect, toward the aromatic ring. This causes a red-shift of the π-π^* transition. Conversely, if a hydrogen bond is formed in which the hydroxyl oxygen is a proton acceptor, electrons are withdrawn from the naphthalene ring, and an opposite shift is anticipated. If both bonds could form at the same time and with equal ease, since their effects on the partial charges of the oxygen are opposite, the net change on the oxygen and hence on the aromatic ring may be small. Therefore, in such a situation, the spectral shift relative to the position of the band in a nonhydrogen-bonding situation ought to be small [65].

The near UV absorption of 1-naphthol which arises from two strongly overlapped π-π^* transitions remain unaffected in the presence of submicellar aqueous CTAB solution, indicating the absence of any appreciable interaction (Figure 4.24). However, interestingly, significant red-shift starts to occur (6.4 nm at λ_{max} ~293 nm) in the presence of CTAB just above its cmc (0.96 mM) with a well-defined isobestic point at 296 nm. Such shifting of λ_{max} continues until most of the naphthol molecules are partitioned in the micellar phase at high surfactant/ naphthol ratio. The absorption spectra of 2-naphthol as a function of CTAB concentration shows similar features but consist of more than one isobestic points (figure 4.25). The result suggests that the protruded OH groups of micelle-embedded naphthols form a H-bond with interfacially located (D_{eff} ~45) water molecules and act as a H-donor. It may also be argued that at a mole ratio of 1:1 of naphthol and the CTAB, at which maximum viscoelastic response is observed under shear, due to the presence of entangled worm-like micelles, not all of the naphthol molecules are embedded in the micelles, but some are located in the stern layer. These naphthols may, however, be involved in H-bond network formation with embedded molecules via interfacial water. The spectral feature and the nature and degree of shift undoubtedly resemble the spectra of 1-naphthol in isooctane at various dioxane concentrations (Figure 4.26) (red-shift of 6.3 nm at λ_{max} ~293 nm,

as compared to a red-shift of 6.4 nm at λ_{max} ~293 nm, Figure 4.24) where naphthol acts as the hydrogen bond donor and dioxane as acceptor [54].

Previously, it has been shown that, in the ground state, 1-naphthol interacts with water via oxygen, whereas with alcohols (ethanol and isopropanol) and acetonitrile it interacts via hydrogen of the hydroxyl group [66]. The nature of spectral modification encountered by micelle free naphthol molecules in the presence of water is shown in figure 4.27. This figure shows that on every addition of water (up to 10% v/v) substantial gain in intensity is displayed by 1-naphthol spectra (in acetonitrile) with little change of wavelength. The nature of spectral modification of 1-naphthol due to H-bond formation is quite different from that of micelle-embedded naphthol. It may be argued that, like alcohols and acetonitrile media, naphthols at the interface (D_{eff} ~45) act as H-donating agents and water as a H-acceptor at the oxygen site. This is indeed interesting. The low D_{eff} value found for the interfacial microenvironment of CTAB micelles may be attributed to a low interfacial water activity. Nevertheless, it has also been argued that the low interfacial D_{eff} value may be a result of the H-bond donor properties of the water in the interfacial region being different from that of bulk water, and/or the presence of electrostatic image interactions caused by the proximity of the low dielectric hydrocarbon core. Present experiments indeed justify the former conjecture precisely [67]. It is known that the water molecules at the micellar interface have some strange properties [68,69]. The solvation dynamics are slowed down by several orders of magnitude relative to bulk water. The reorientational motion is also restricted. The dynamics of water molecules near an aqueous micellar interface has been a subject of intense current interest because such a system serves as a prototype of complex biological system. Furthermore, oxygen K absorption and emission spectra of water molecules in the micellar interface also show that the local electronic structure of water molecules is dramatically different from that of bulk water [70]. The relatively less polar and less mobile water molecules compared to bulk water form a strong H-bond with the OH group of embedded naphthols, which act as H-donors and result in an optimum orientation of aromatic π-electron systems in the micelles to shield the surfactant headgroup charges efficiently; maybe via cation-π interaction; i.e., cation charge of surfactant

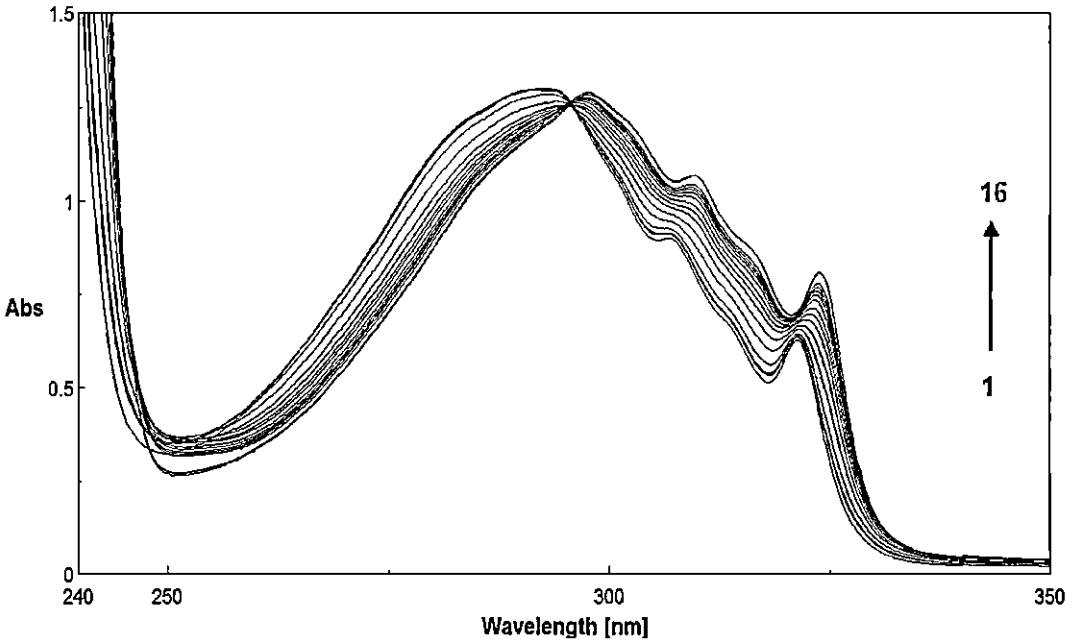

Figure 4.24. Absorption spectra of 1-Naphthol (0.25 mM) in water at varying concentrations of CTAB at 25 °C. [CTAB]: (1) 0.0, (2) 0.44, (3) 0.55, (4) 0.75, (5) 1.00, (6) 1.25, (7) 1.50, (8) 1.75, (9) 2.00, (10) 2.50, (11) 3.00, (12) 3.50, (13) 4.00, (14) 5.00, (15) 15.00, (16) 20.00 mM.

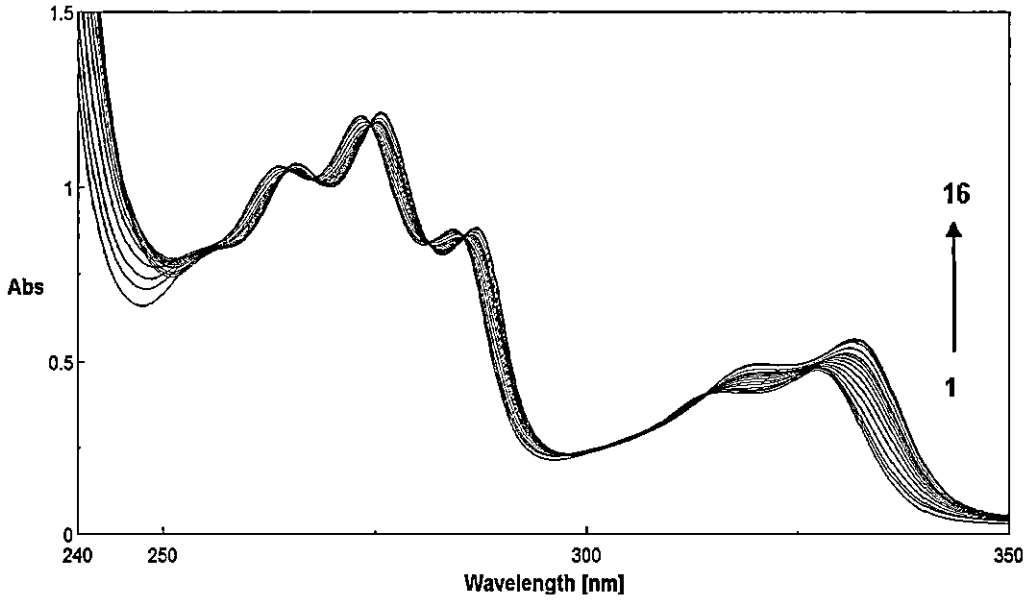

Figure 4.25. Absorption spectra of 2-Naphthol (0.25 mM) in water at varying concentrations of CTAB at 25 °C. [CTAB]: (1) 0.0, (2) 0.65, (3) 0.79, (4) 0.94, (5) 1.13, (6) 1.36, (7) 1.63, (8) 1.96, (9) 2.35, (10) 2.82, (11) 3.39, (12) 5.08, (13) 7.63, (14) 11.44, (15) 17.16, (16) 20.60 mM.

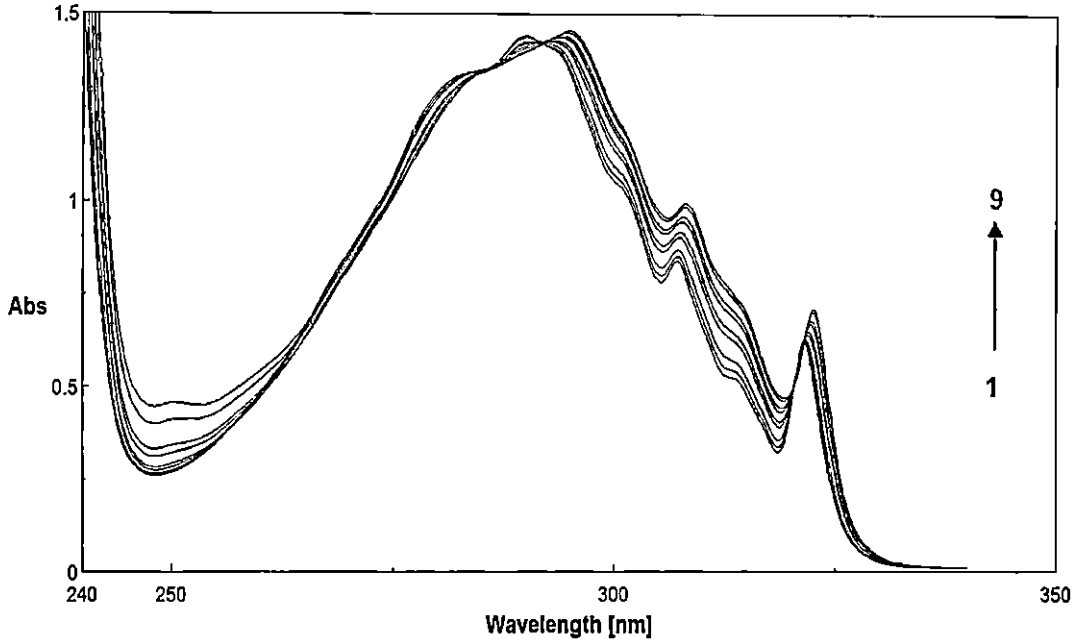

Figure 4.26. Absorption spectra of 1-Naphthol (0.25 mM) in isooctane at varying concentrations of 1,4-dioxane at 25 °C. [Dioxane]: (1) 0.0, (2) 13, (3) 20, (4) 40, (5) 50, (6) 80, (7) 100, (8) 160, (9) 200 mM.

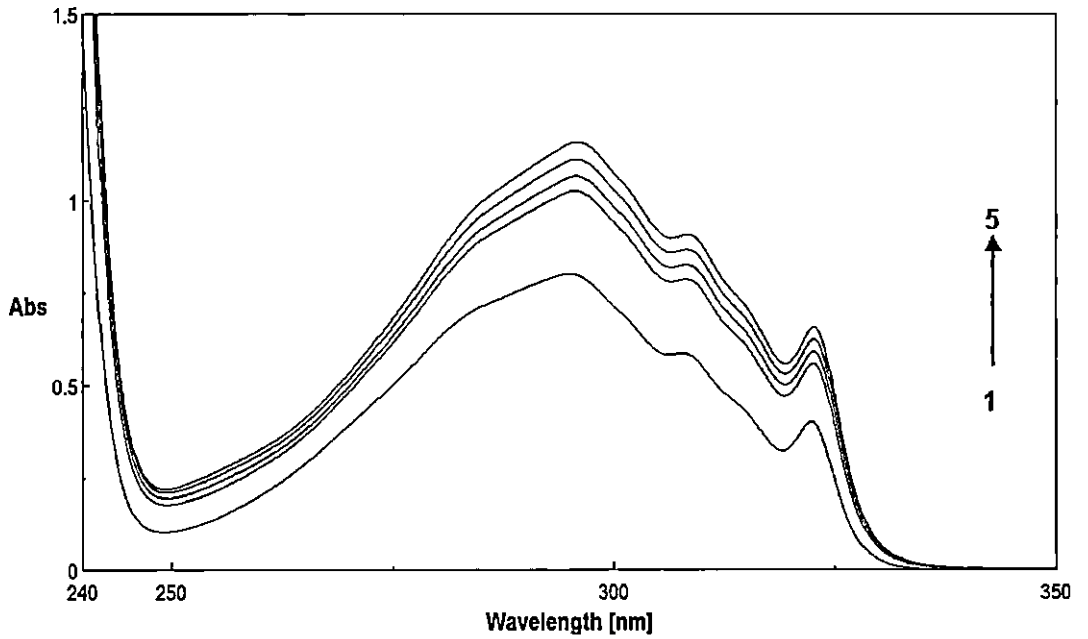

Figure 4.27. Absorption spectra of 1-Naphthol (0.25 mM) in acetonitrile at different percentages of water at 25 °C. % of water: (1) 0.00 %, (2) 4.00 %, (3) 6.00 %, (4) 8.00 %, (5) 10.00 %.

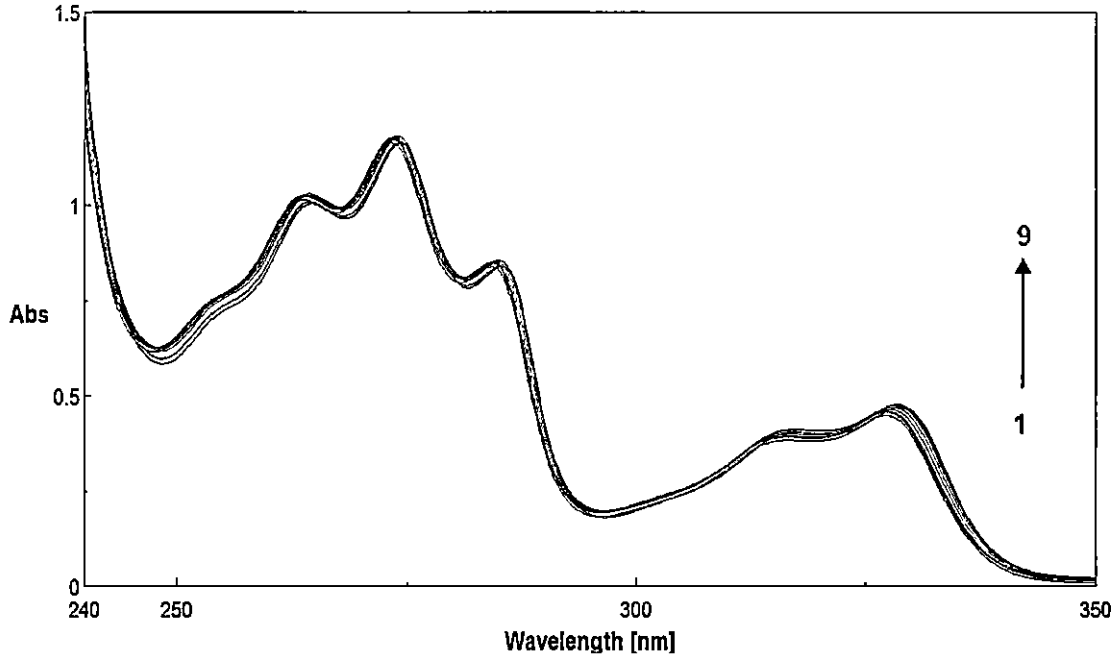

Figure 4.28. Absorption spectra of 2-Naphthol (0.25 mM) at varying concentrations of SDS in water at 25 °C. [SDS]: (1) 0.0, (2) 5.6, (3) 6.91, (4) 8.30, (5) 9.96, (6) 11.95, (7) 14.34, (8) 17.21, (9) 30.97 mM.

head groups interacts with the quadrupole moment of the aromatic π-system of naphthols. Cation-π interaction energies are of the same order of magnitude as hydrogen bonds and play an important role in molecular recognition [58]. To further strengthen the above view (involvement of cation-π interaction), the absorption spectra of the naphthols were recorded in aqueous SDS of varying concentrations. The possibility of a cation-π interaction in SDS can directly be ruled out due to the anionic head group of the surfactant. Figure 4.28 shows the absorption spectra of 2-naphthol in aqueous SDS. As expected, no appreciable shift at any of the vibrational bands of the probe molecule was observed. Moreover, very small enhancement in the absorbance of the peaks was seen.

On the other hand, as the H atom of OH is replaced by a CH_3 group (viz., the methoxynaphthalene molecules), the ability of intermolecular H-bond formation disappears. Instead, the H-accepting tendency from a potential donor is enhanced. The absorption spectra of 1- and 2- methoxynaphthalene in aqueous CTAB are shown in figures 4.29 and figure 4.30 respectively. The nature of changes

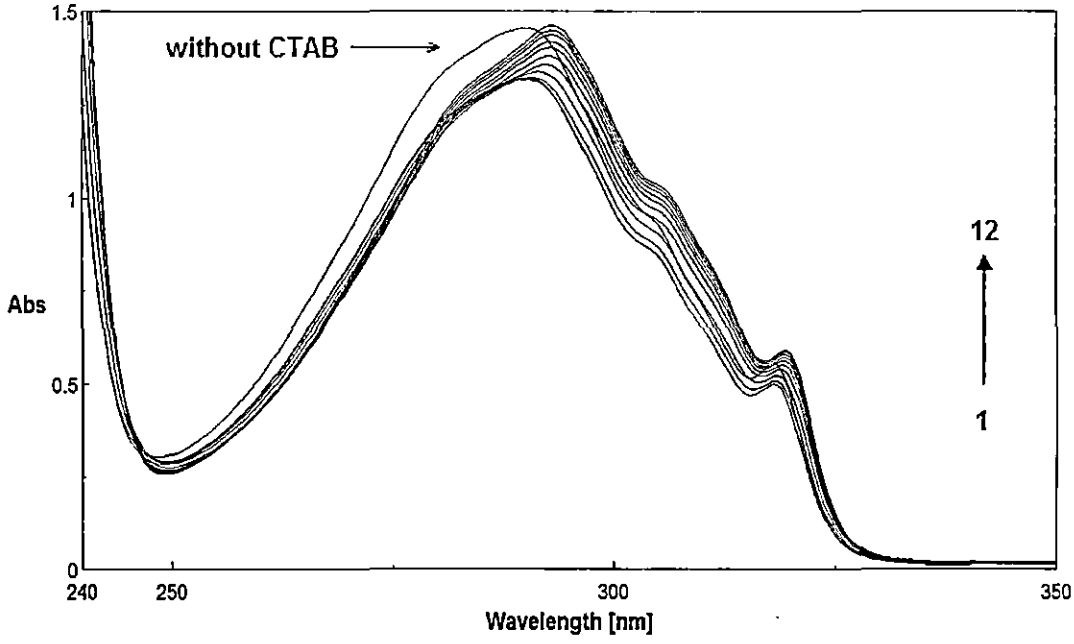

Figure 4.29. Absorption spectra of 1-Methoxynaphthalene (0.25 mM) in water at varying concen-trations of CTAB at 25 °C. [CTAB]: (1) 0.0, (2) 0.33, (3) 0.55, (4) 0.75, (5) 1.00, (6) 1.50, (7) 2.00, (8) 2.50, (9) 3.00, (10) 3.50, (11) 4.00, (12) 5.00 mM.

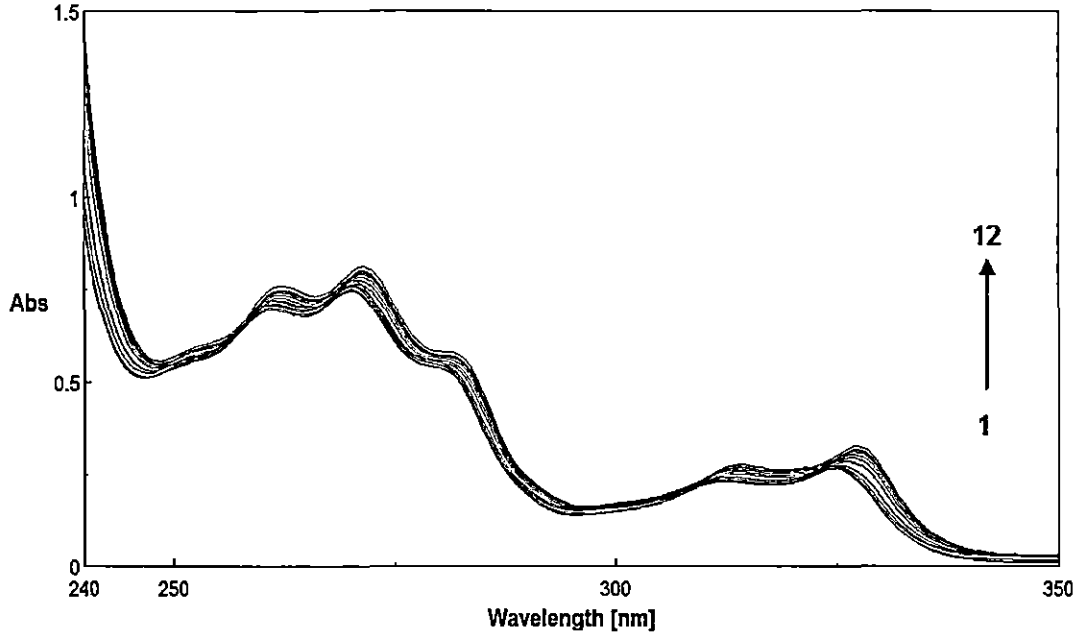

Figure 4.30. Absorption spectra of 2-Methoxynaphthalene (0.25 mM) in water at varying concent-rations of CTAB at 25 °C. [CTAB]: (1) 0.0, (2) 0.33, (3) 0.50, (4) 0.75, (5) 1.00, (6) 1.50, (7) 2.00, (8) 2.50, (9) 3.00, (10) 3.50, (11) 4.00, (12) 5.22 mM.

encountered in the UV spectra of 1- and 2- methoxynaphthalene on the addition of CTAB above its cmc indicates the permeation of the probe molecules in the micelles. The small red-shift, with the absence of any isobestic point(s), compared to that in naphthols indicates that a weaker noncovalent interaction takes place. The large drop in intensity on first addition of 0.33 mM CTAB is the signature of breaking of H-bonds with bulk water molecules. To examine the stabilities of the hydrogen bonding and the cation-π interactions in the 1-naphthol/CTAB and 1-methoxynaphthalene/CTAB systems respectively, the absorption spectra were recorded at higher temperatures. Interestingly, the spectra of 1-naphthol/CTAB system at 70°C (figure 4.31) shows dentical features as that at 25°C. Moreover, the shift in the λ_{max} is also the same (as that at 25°C). Therefore, it may be argued that the H-bonds which are formed at the interface are strong and remain stable even at 70°C. On the other hand, the 1-methoxy-naphthalene/CTAB system, with only cation-π interactions, behave differently even at 50°C (compared to that at 25°C). The spectra of probes show only gain in intensity on addition of surfactants (with negligible shift at the maximum wavelength) due to the increasing presence of non polar environment in the micellar phase (figure 4.32).

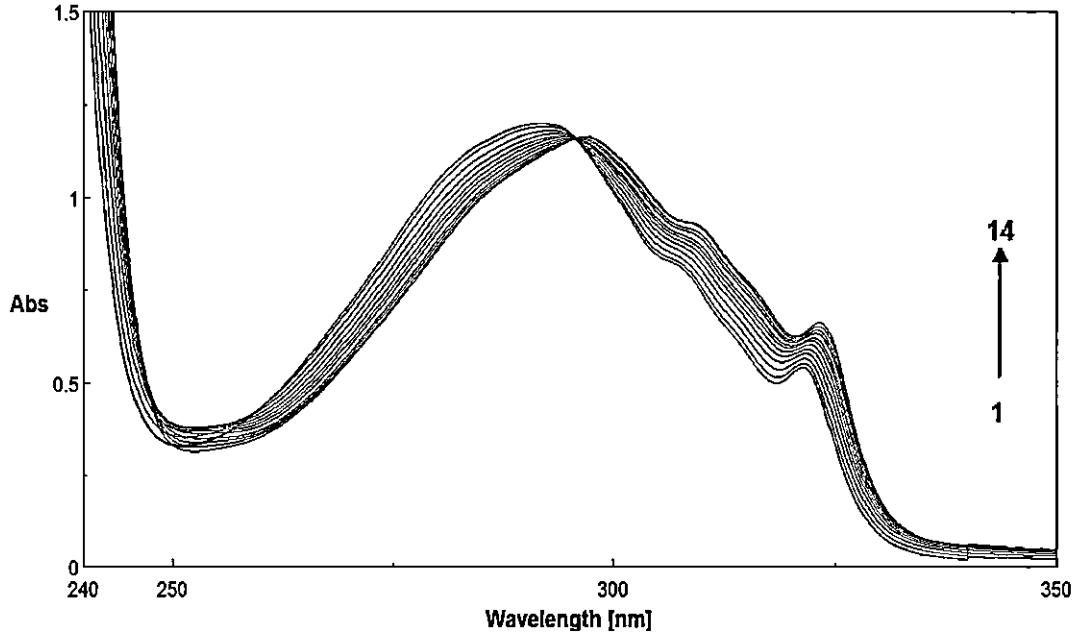

Figure 4.31. Absorption spectra of 1-Naphthol (0.25 mM) in water at varying concentrations of CTAB at 70 °C. [CTAB]: (1) 0.0, (2) 0.73, (3) 0.98, (4) 1.31, (5) 1.63, (6) 2.04, (7) 2.56, (8) 3.2, (9) 4.00, (10) 5.00, (11) 7.50, (12) 10.00, (13) 15.00, (14) 20.30 mM.

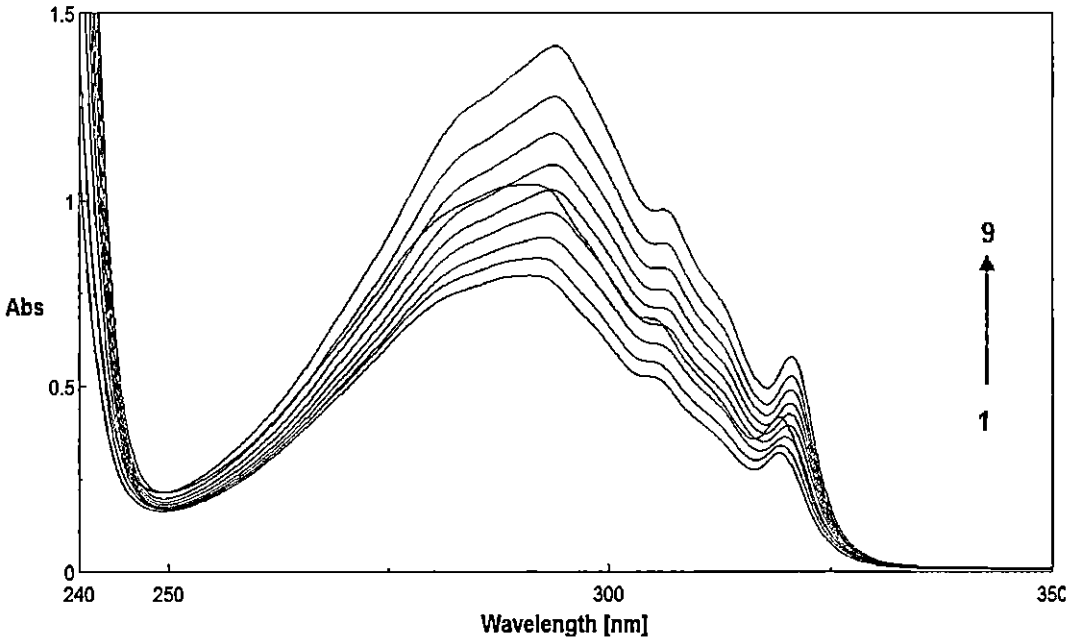

Figure 4.32. Absorption spectra of 1-Methoxynaphthalene (0.25 mM) in water at varying concen-trations of CTAB at 50°C. [CTAB]: (1) 0.52, (2) 0.78, (3). 1.75, (4) 2.63, (5) 3.95, (6) 5.92, (7) 8.88, (8) 13.33, (9) 20.00 mM.

Due to their directionality and spatial arrangement, complementary multiple H-bonding interactions at the micellar interface lead to engineering well-defined supramolecular structure via micellar headgroup charge shielding by π-electron systems of naphthols (Figure 4.33). This result of unusual H-bonding may be relevant, not only when considering the H-bonding of the interfacial water molecules in the specific micelle and dopant studied here but also for the H-bonding interaction of other micelle-dopant systems as well. Therefore, unlike methoxynaphthalenes, naphthols interact with micelles strongly and the UV spectra of naphthols are modified showing significant red-shifting and display sharp isobestic point due to strong H-bonding interaction with interfacial water molecules.

The spectral modifications of the probe molecules in CTAB micelles (with C_{16} hydrocarbon chain), promted to extend the spectroscopic investigation with other members of the alkyltrimethylammonium bromide series, viz; DTAB (C_{12}) and TTAB (C_{14}). It is well known that the compactness of the head group of the alkyltrimethylammonium surfactants increase with an increase in the surfactant

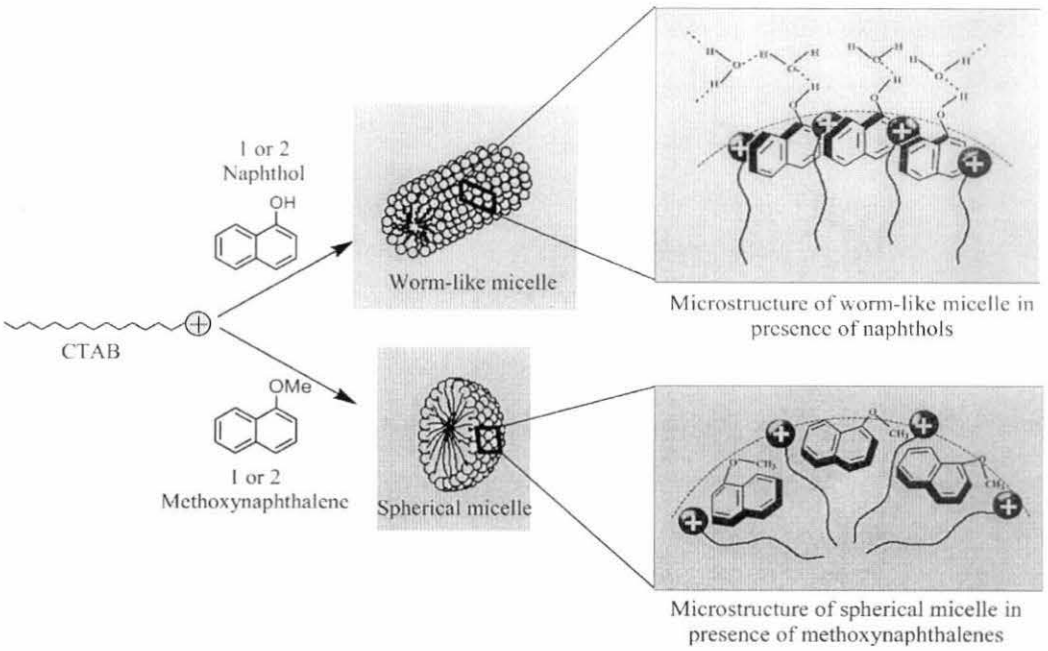

Figure 4.33. Schematic representation of the microstructures found in worm-like micelles formed by naphthols and spherical micelles formed by methoxynaphthalenes with CTAB.

chain length. Neutron scattering experiments on micelles having different surfactant chain lengths reveal that the head group structures of the micelles differ significantly [71,72]. For example, in DTAB water penetrates into the head group region to a depth of ~4 carbons, whereas in TTAB water penetrates to a depth of ~2.5 carbons [73]. Therefore, to check the effect of surfactant chain length and the validity of the water penetration (micellar hydration) model on the absorption characterstics of the hydroxynaphthalenes, studies with DTAB and TTAB were also carried out in aqueous media (figures 4.34 to 4.37). Interestingly, shifts in the maximum wavelengths of the probe molecules are the same irrespective of the hydrocarbon chain length of the surfactants. For example, the longest wavelength band of 1-naphthol in water which arises at 321.2 nm shifts to a maximum of 323.8 nm in presence of 10 mM CTAB. At this concentration all the naphthols are supposed to be fully bound to the CTAB micelles. The same shift is also observed for the probe molecule in micelles of TTAB and DTAB when fully bound. Moreover, the position of the isobestic point too remains unmoved with changes in the hydrophobicity of the surfactant. Arguing in line with the water penetration

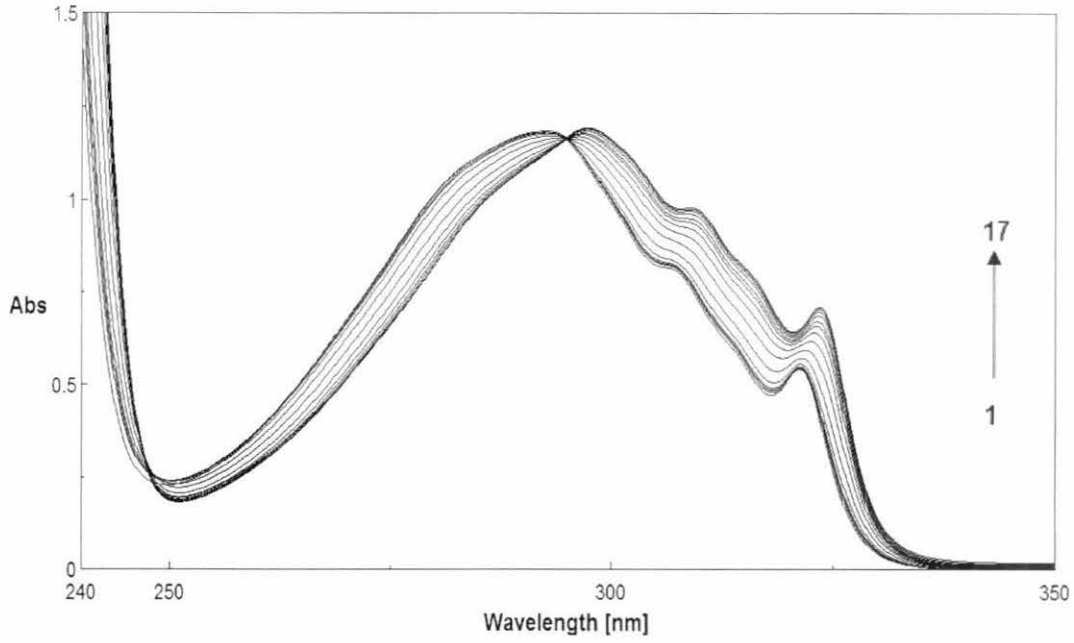

Figure 4.34. Absorption spectra of 1-Naphthol (0.25 mM) in water at varying concentrations of DTAB at 25 °C. [DTAB]: (1) 0.0, (2) 8.40, (3) 10.08, (4) 11.00, (5) 12.00, (6) 13.09, (7) 14.28, (8) 15.58, (9) 17.00, (10) 18.55, (11) 20.24, (12) 24.29, (13) 29.15, (14) 34.98, (15) 41.98, (16) 50.37, (17) 60.45 mM

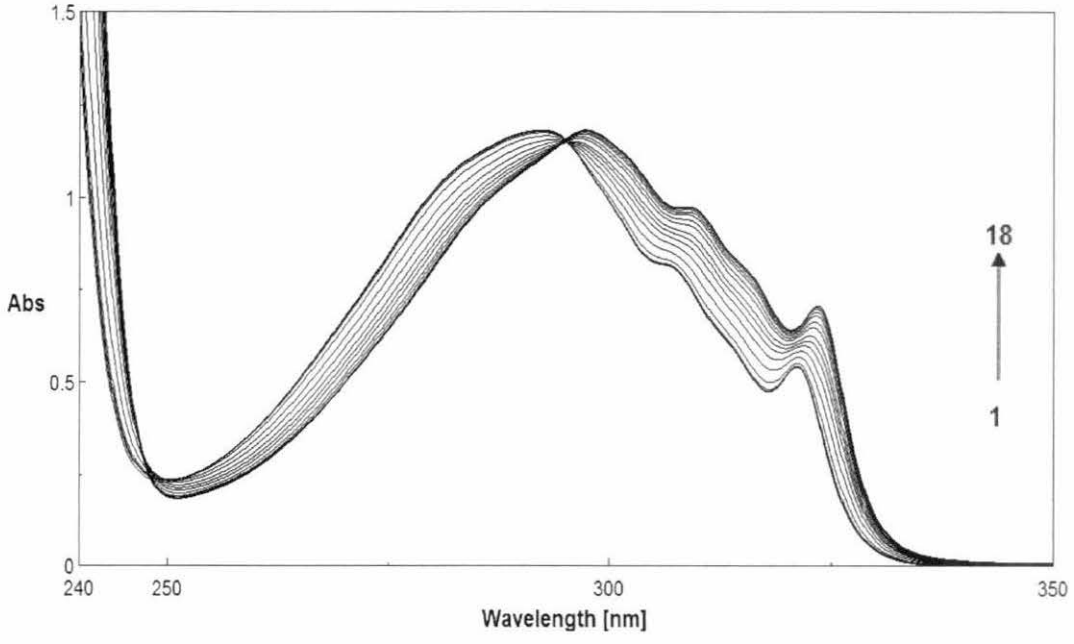

Figure 4.35. Absorption spectra of 1-Naphthol (0.25 mM) in water at varying concentrations of TTAB at 25°C. [TTAB]: (1) 0.0, (2) 1.96, (3) 2.62, (4) 3.15, (5) 3.43, (6) 3.75, (7) 4.09, (8) 4.47, (9) 4.87, (10) 5.32, (11) 6.39, (12) 7.67, (13) 10.23, (14) 13.64, (15) 18.19, (16) 24.26, (17) 29.11, (18) 39.94 mM

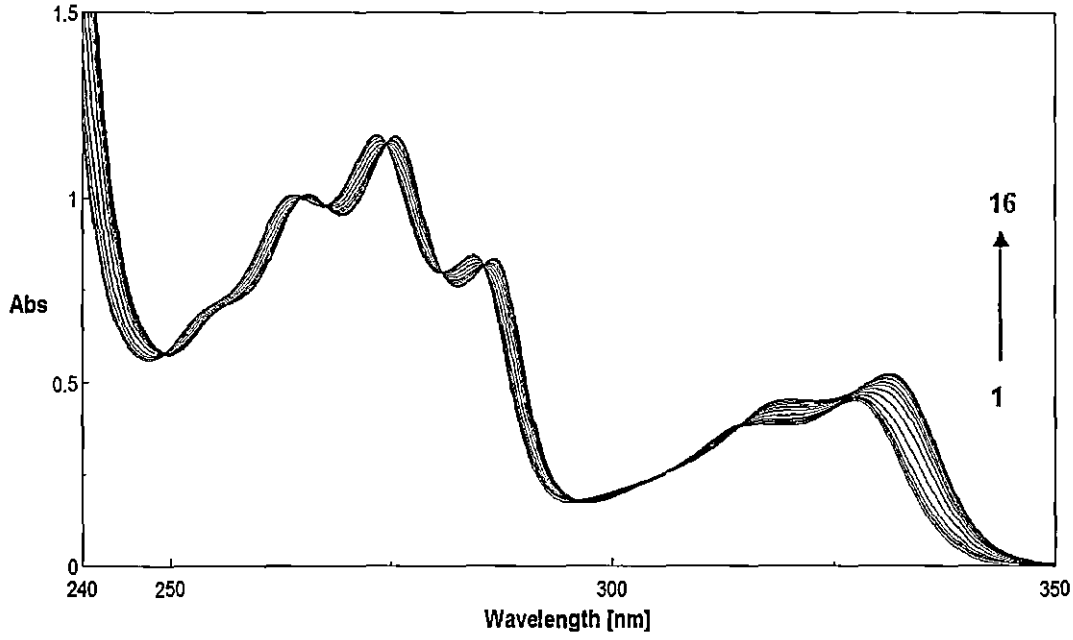

Figure 4.36. Absorption spectra of 2-Naphthol (0.25 mM) in water at varying concentrations of DTAB at 25 °C. [DTAB]: (1) 0.0, (2) 8.31, (3) 9.97, (4) 11.96, (5) 13.05, (6) 14.24, (7) 15.53, (8) 16.94, (9) 18.49, (10) 20.17, (11) 24.22, (12) 29.05, (13) 34.86, (14) 41.84, (15) 50.21, (16) 60.26 mM.

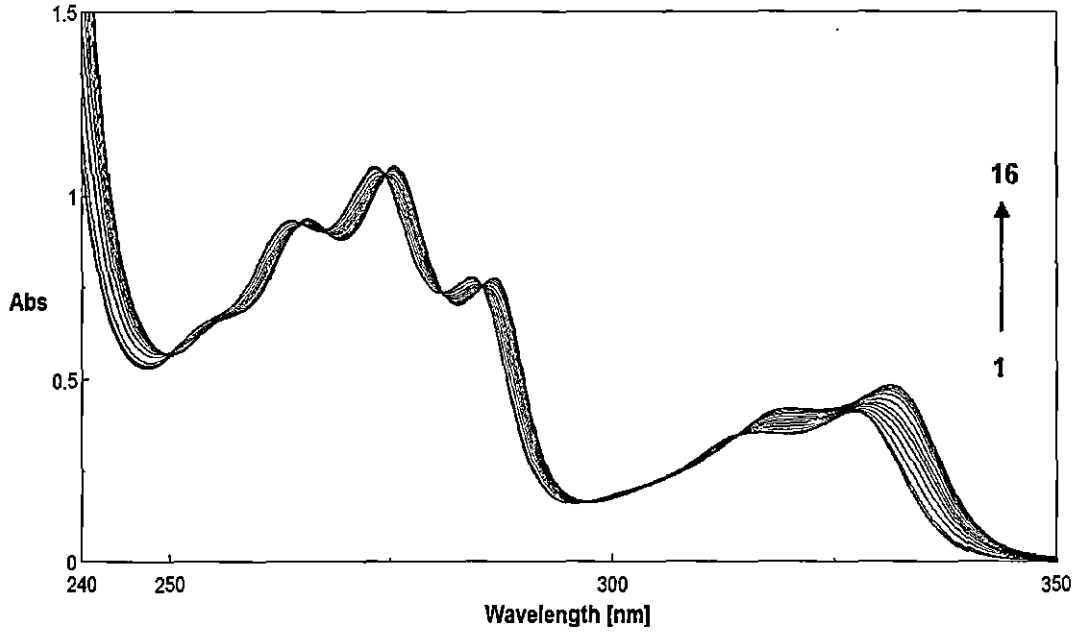

Figure 4.37. Absorption spectra of 2-Naphthol (0.25 mM) in water at varying concentrations of TTAB at 25°C. [TTAB]: (1) 0.0, (2) 2.33, (3) 2.80, (4) 3.36, (5) 3.67, (6) 4.01, (7) 4.37, (8) 4.77, (9) 5.21, (10) 6.25, (11) 8.33, (12) 11.11, (13) 14.81, (14) 19.75, (15) 26.33, (16) 31.60 mM.

penetration model, the increased micellar hydration in DTAB (as compared to TTAB and CTAB) would have caused lesser spectral shifts because the microenvironment faced by the probe in DTAB micelles would be more polar. This was however, not observed. From the foregoing observations we conclude that the spectral modification of the hydroxynaphthalenes (both 1- and 2-naphthols) in cationic micelles of alkyltrimethylammonium bromides is solely a consequence of hydrogen bonding with the interfacial water molecules in combination with cation-π interactions and that other factors like micellar hydration and temperatures seems insignificant.

4.3.4.3. Spectral modifications of Dihydroxyaromatic compounds in micellar media

While both the monohydroxynaphthalenes (1- and 2-naphthols) imparts strong viscoelasticity in the solution of CTAB micelles, the behaviour of the dihydroxynaphthalenes (DHN), viz., 2,3-dihydroxynaphthalene and 2,7-dihydroxynaphthalene towards micellar solutions of CTAB is quite different. 2,3-dihydroxynaphthalene when mixed with aqueous CTAB, formed a viscoelastic gel, the maximum viscosity occurring at a mole ratio of 1:1 (figure 4.2). On the other hand 2,7-dihydroxynaphthalene could not form viscoelastic solutions with CTAB. Therefore, spectroscopic investigation of the dihydroxy dopants in aqueous CTAB have been carried out. The effect of other alkyltrimethylammonium bromides (DTAB and TTAB) on the absorption properties of 2,3 and 2,7 - dihydroxynaphthalenes have also been investigated.

The near-UV absorption spectrum of 2,3 and 2,7-DHN exhibits several sharp vibrational components among which the longest wavelength band, the π-π^* band arises mainly due to the $^1L_b \leftarrow {}^1A$ transition. The interaction of alkyltrimethylammonium bromide surfactants with 2,3 and 2,7-DHN were studied at several concentrations range so as to cover both the submicellar and post micellar regions. Unlike 1 and 2-naphthols, where the absorbance remained constant upto the cmc of the added surfactant, the absorbance at the longest wavelength band of 2,3 and 2,7-DHN (324 nm for 2,3-DHN and 325.6 nm for 2,7-

DHN) experienced an initial sharp decrease with increasing CTAB concentration. The decrease in absorbance at 324 nm continued upto the cmc of the surfactant and then a sharp rise in the absorbance with a red-shift of ~3.0 nm is observed. The absorption spectra of 2,3-DHN in aqueous CTAB is shown in figure 4.38. Well defined isobestic points at 282, 307.1, 311.2, 321 and 324 nm shows that equilibrium between the micelle bound and the free probe molecules exists. The longest wavelength band at 324 nm undergoes a gradual blurring of vibrational fine structure with a significant red shift (~3 nm). Although blurring or broadening occurs in the vibrational structure, there exists a similarity between the spectra of the free and the micelle embedded molecules. The blurring of vibrational structure and the shift to longer wavelength continues only upto a concentration of 5 mM CTAB and beyond 5 mM, the loss of vibrational structure is regained and no further shift in the λ_{max} is observed indicating that the probes are being increasingly incorporated within the micelles. Therefore, at a concentration of 5 mM all the 2,3-DHN molecules are fully embedded in the micelles and are hydrogen bonded with the interfacial water molecules surrounding the micelles. Previously, a similar red-shift of absorption spectra band of 2-naphthol in AOT reverse micelle was observed, where AOT acts as hydrogen-bond donor and the perturbation on π electrons caused by the negative charge carried on oxygen atom of the partner molecule due to H-bonding occurs [74]. The same reasoning applies to the present case also and the nature of spectral change indicates in favour of H bonding between dihydroxy naphthalene molecules which are embedded increasingly in the micelle as the CTAB concentration (>1.0 mM) is increased. The spectra of 2,7-DHN/CTAB system showed similar red shifts with isobestic points at 293.4, 323.6 and 326.9 nm only (figure 4.39). The absorption spectra of 2,3-DHN and 2,7-DHN in aqueous solutions of DTAB and TTAB are shown in figures 4.40 to 4.43. Though 2,3-DHN and 2,7-DHN produces completely different effects on CTAB micelles, for instance, 2,3-DHN induces microstructural transition from spherical to worm-like micelles and imparts strong viscosity to CTAB solutions but 2,7-DHN does not, not much difference in the absorption pattern is observed. The only difference in the spectral features of the two dihydroxy naphthalenes lies in the number of isobestic points (5 for 2,3-DHN and 3 for 2,7-DHN). Nevertheless

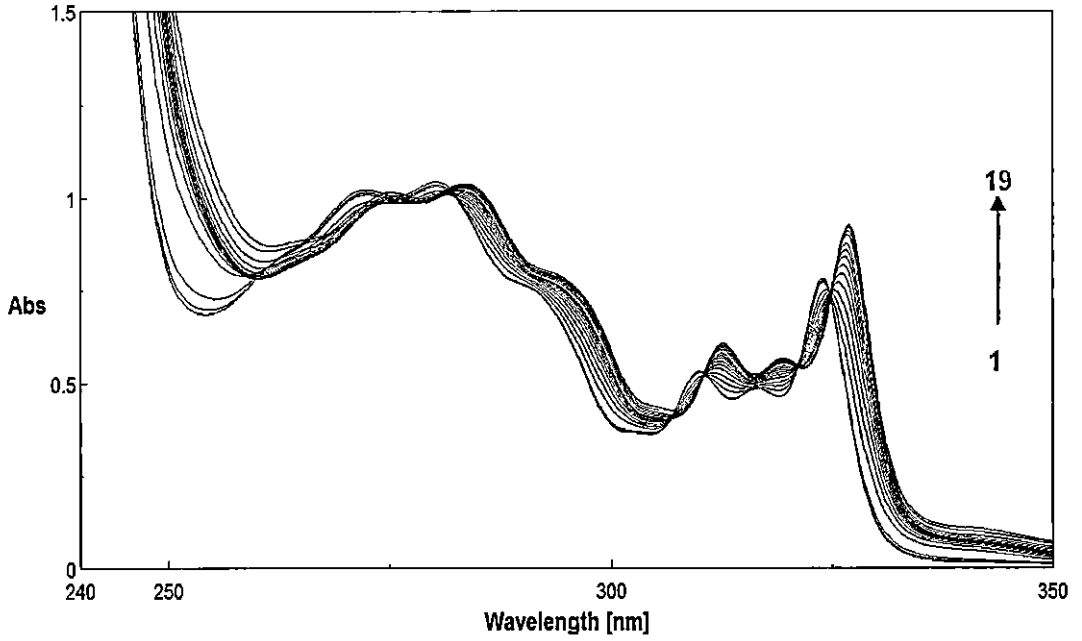

Figure 4.38. Absorption spectra of 2,3-dihydroxynaphthalene (0.25 mM) in water at varying concen-trations of CTAB at 25°C. [CTAB]: (1) 0.00, (2) 0.41, 0.61, (3) 0.61, (4) 0.92, (5) 1.10, (6) 1.32, (7) 1.59, (8) 1.91, (9) 2.29, (10) 2.75, (11) 3.30, (12) 3.96, (13) 5.94, (14) 7.92, (15) 10.56, (16) 14.08, (17) 18.78, (18) 25.04, (19) 30.05 mM

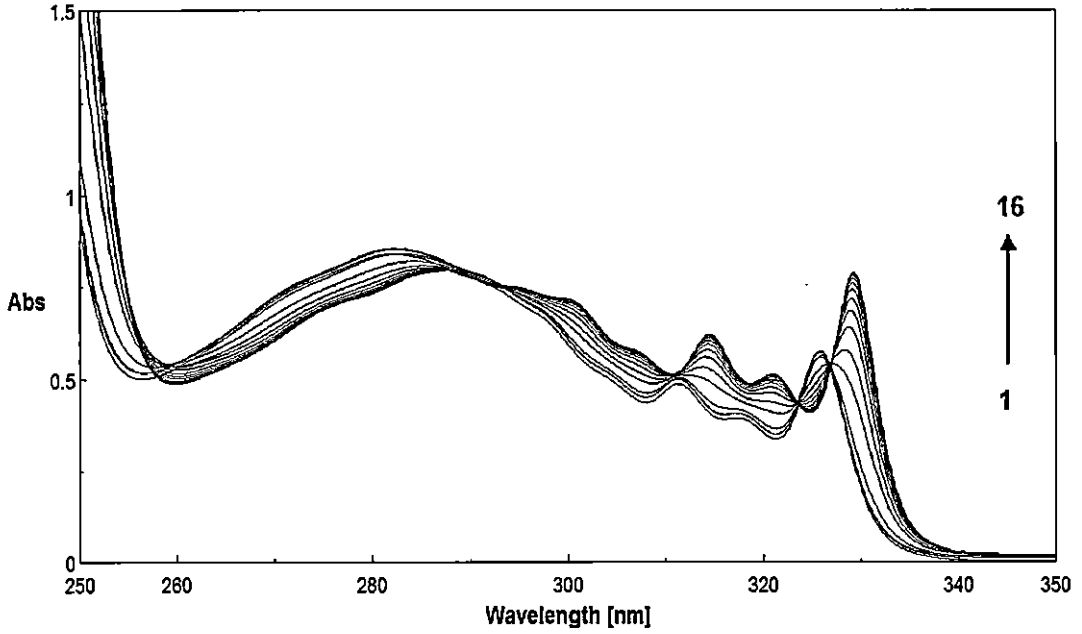

Figure 4.39. Absorption spectra of 2,7-dihydroxynaphthalene (0.25 mM) in water at varying concen-trations of CTAB at 25°C. [CTAB]: (1) 0.00, (2) 0.37, (3) 0.56, (4)0.84, (5) 1.27, (6) 1.69, (7) 2.25, (8) 3.00, (9) 4.00, (10) 5.34, (11) 7.12, (12) 9.49, (13) 12.65, (14) 16.87, (15) 22.50, (16) 30.10 mM

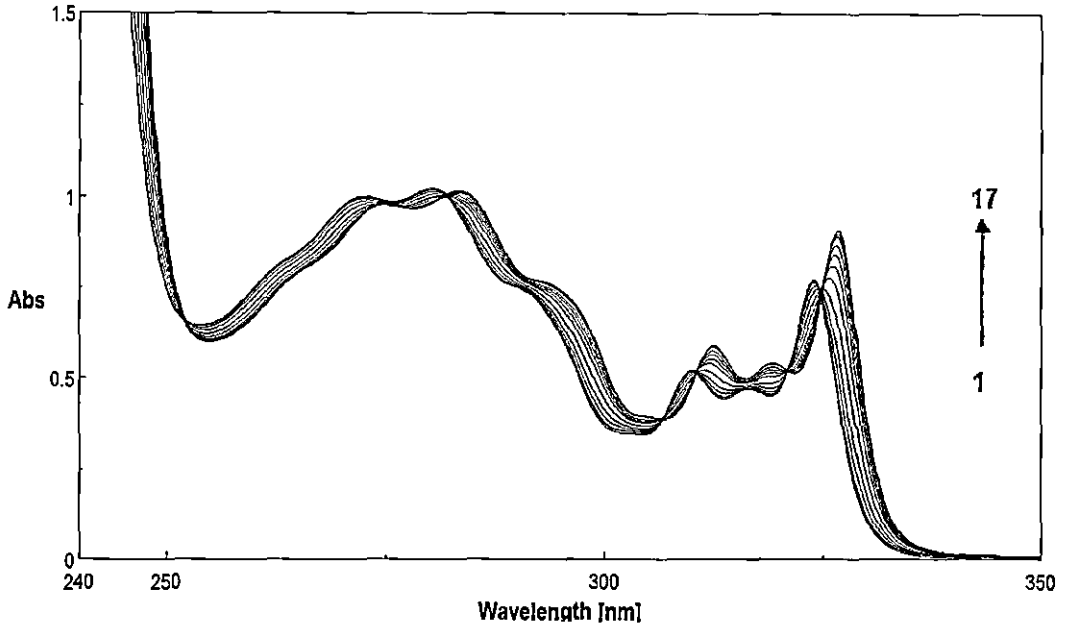

Figure 4.40. Absorption spectra of 2,3-dihydroxynaphthalene (0.25 mM) in water at varying concen-trations of DTAB at 25°C. [DTAB]: (1) 0.00 , (2) 6.92, (3) 8.31, (4) 9.97, (5) 11.96, (6) 13.05, (7) 14.24, (8) 15.53, (9) 16.95, (10) 18.49, (11) 20.17, (12) 24.20, (13) 29.05, (14) 34.86, (15) 41.84, (16) 50.20, (17) 60.25 mM

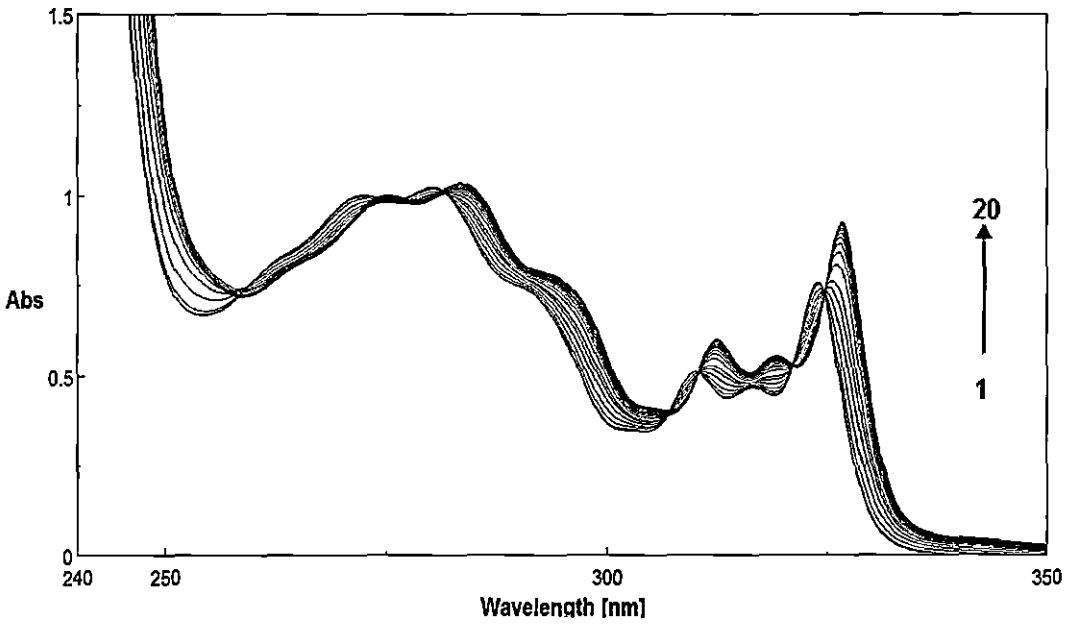

Figure 4.41. Absorption spectra of 2,3-dihydroxynaphthalene (0.25 mM) in water at varying concen-trations of TTAB at 25°C. [TTAB]: (1) 0.00 , (2) 1.78 , (3) 2.67, (4) 3.21, (5) 3.50, (6) 3.82, (7) 4.16, (8) 4.54, (9) 5.45, (10) 6.54, (11) 7.85, (12) 9.42, (13) 11.31, (14) 13.57, (15) 16.29, (16) 19.54, (17) 23.45, (18) 28.15, (19) 33.78, (20) 40.53 mM

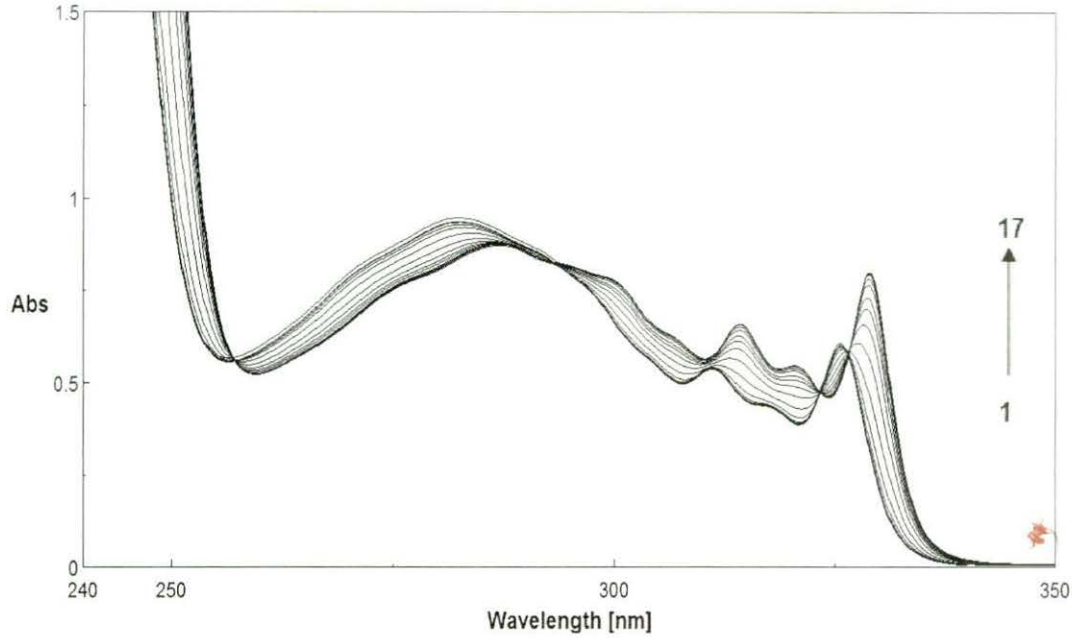

Figure 4.42. Absorption spectra of 2,7-dihydroxynaphthalene (0.25 mM) in water at varying concen-trations of DTAB at 25°C. [DTAB]: (1) 0.00 , (2) 6.23, (3) 8.31, (4) 9.97, (5) 11.96, (6) 13.05, (7) 14.24, (8) 15.53, (9) 16.95, (10) 18.49, (11) 20.17, (12) 24.20, (13) 29.04, (14) 34.85, (15) 41.82, (16) 50.19, (17) 60.23 mM

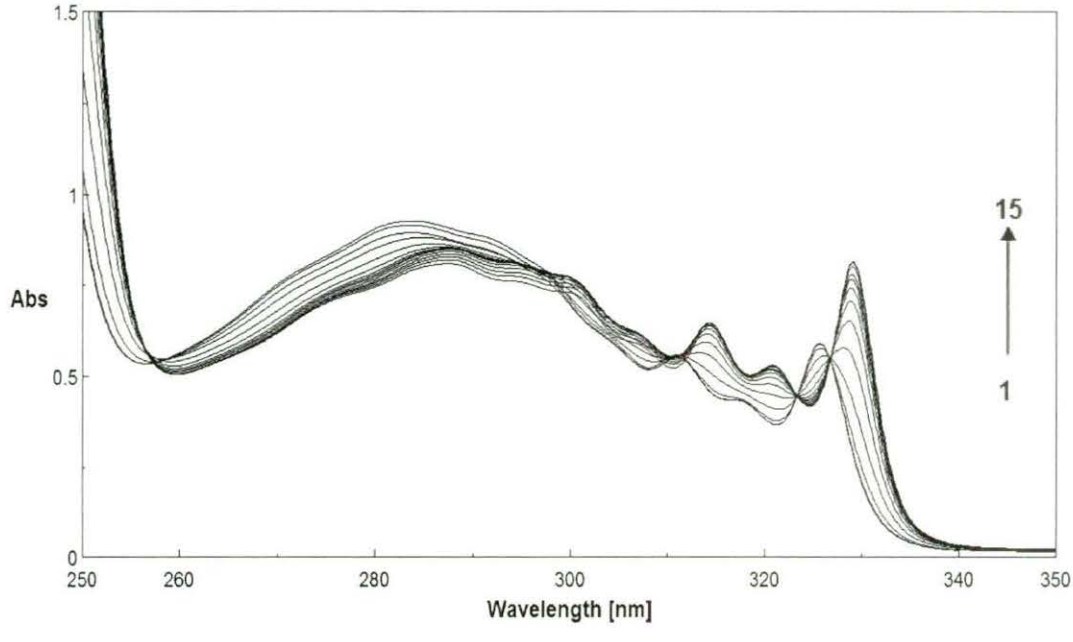

Figure 4.43. Absorption spectra of 2,7-dihydroxynaphthalene (0.25 mM) in water at varying concen-trations of TTAB at 25°C. [TTAB]: (1) 0.00 , (2) 1.56, (3) 2.09, (4) 2.79, (5) 3.35, (6) 4.02, (7) 4.82, (8) 5.78, (9) 6.94, (10) 8.33, (11) 10.00, (12) 15.00, (13) 21.38, (14) 25.66, (15) 30.80 mM

the result strongly indicates the presence of hydrogen bonding (as discussed for the naphthol/CTAB), between the micelle bound dopants and the surrounding interfacial water molecules.

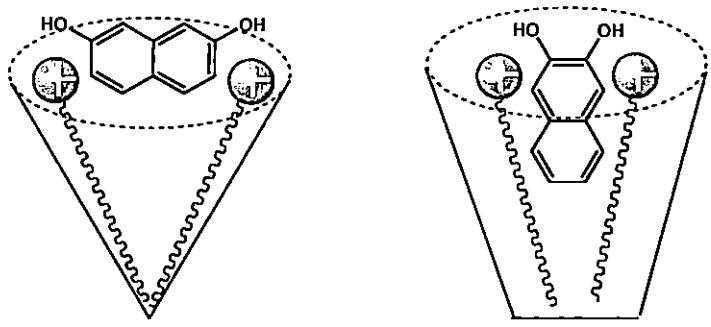

Figure 4.44. Schematic representation of the location and position of 2,3-DHN and 2,7-DHN in CTAB micelles.

From the above discussions, and the results obtained from ^{1}H NMR studies, the location and position of both the dihydroxynaphthalenes in micelles of CTAB can be understood. The schematic representation of the probable microstructure of the micelle in presence of the dopants is shown in figure 4.44. Because the polar hydroxyl groups must keep a certain contact with water, the positions of the hydroxyl groups in the naphthalene ring of 2,7-DHN prevents the ring from penetrating deeper into the micellar core. However, for 2,3-DHN the positions of the OH groups favour the entry of the hydrophobic aromatic part deep inside the micelle due to hydrophobic interactions. Thus, the packing of the 2,7-DHN /CTAB system should be less tight than for the 2,3-DHN/CTAB. The critical packing parameter of the 2,3-DHN/CTAB system most probably exceeds 1/3 and microstructural transition from micelles to worm like micelles take place in presence of strong cation- π interaction. On the other hand, such a possibility is remote in 2,7-DHN/CTAB system and the packing parameter value does not exceed 1/3. This corroborates the strong influence of the hydroxyl group, which apparently changes the orientation of the naphthalene ring at the micellar surface. Thus, unlike the hydroxynaphthalenes, the position of OH groups in dihydroxy-naphthalenes seems to be a decisive factor in the microstructural transiton of the micelles.

4.3.5. Surfactant Probe Binding Equilibrium

The enhancement of absorbance of the probe molecules in micellar solutions of alkyltrimethylammonium bromides can be rationalised in terms of binding of the probe with the micelle. As has already been mentioned, the most significant property of an organised assembly in spectroscopy is its ability to stabilise and bind solute molecules that are typically insoluble or sparingly soluble in bulk neat solvent [56]. However, the strength of binding can be identified through the determination of binding constant derived from the equilibrium between the probes and the micelle. Plots of absorbance at the longest wavelength band of all the dopants, against the concentrations of the surfactants, show discontinuity at two critical points, one at the cmc and the other at the concentration beyond which no change in the position of the longest λ_{max} is observed. However, at concentrations between the two critical points, the curves are linear. For DTAB, linear plots are obtained between 14.6 to 20.0 mM and for TTAB and CTAB the linear portions are between 3.3 to 6.3 mM and 0.95 to 3.1 mm respectively. Hence, only the linear portions of the curve have been utilized to determine the binding constant in the present investigation. For the monohydroxy naphthalenes (1 and 2-naphthols) the values of the absorbance remains almost steady upon initial addition of surfactant, below the cmc, and then increases sharply and finally levels off to a plateau. The values of the absorbance of the probes in water and in presence of various concentrations of surfactants are utilized to obtain the strength of the binding between the two. The variation of absorbance of the monohydroxynaphthalenes (1- and 2-naphthols) and dihydroxynaphthalenes (2,3 and 2,7 -dihydroxynaphthalenes) against the concentration of the surfactants, viz; DTAB, TTAB and CTAB are shown in figure 4.45 to figure 4.56. It is interesting to note that the concentration from which a sharp rise in absorbance is observed, corresponds to the cmc of the individual surfactants. Therefore, the hydroxyaromatic compounds of the present investigation can serve to be potential probes for the determination of the critical micellisation concentrations as well. The values of cmc thus obtained are presented in table 4.1. As can be seen from figures 4.51 to 4.56, the dihydroxy naphthalenes (2,3-DHN and 2,7-DHN) too show break in the absorbance versus concentration plots. The values first decrease to a

minimum and then increases. The minimum value is taken as the cmc of the surfactant. The values of cmc reported here are in good agreement with those reported in the literature [75, 76].

The binding constant K_s's (and surfactant c.m.c.'s) of the individual probe molecules, namely 1-naphthol, 2-naphthol, 2,3-dihydroxy-naphthalene and 2,7-dihydroxy-naphthalene along with the methoxynaphthalenes with alkyltrimethylammonium bromide micelles are determined from the study of the effect of added surfactant on the absorption spectra of the dopants using the following relationships:

$$f / (1-f) = K_s \{ [D] - [S]_t f \} - K_s \text{ cmc.}$$

Where, $f = [S_m] / [S_t]$ and $D_m = [D_t] - \text{cmc}$ (suffix t refers to total). Above equation is drawn assuming following equilibrium to hold between aqueous solubilisate (S_w) and the surfactant (D_m) to form the micelle embedded substrate (S_m),

$$S_w + D_m = S_m$$

Experimentally, f is calculated by, $f = (A - A_w) / (A_m - A_w)$, where A, A_w, and A_m are absorption intensities in surfactant, in water and at complete micellization of substrate, respectively. A plot of $f/(1-f)$ against $([D] - [S]_t f)$ shows discontinuity at two critical points (as mentioned above). The plot of $f/(1-f)$ against $([D] - [S]_t f)$ for the probe molecules in DTAB, TTAB, and CTAB gives good straight lines, from the slope of which the binding constant K_s is obtained. The plots utilized to obtain the binding constant values are shown in the inset of figures 4.45 to 4.56. The values of the binding constants with micelles of DTAB, TTAB and CTAB and the dopants are listed in table 4.1. The binding constants of the probe molecules with the surfactants increase with the increase in the chain length of the micelle and follow the order CTAB > TTAB > DTAB. Increase in the hydrocarbon chain length of surfactant increases the compactness of the micelle which in turn favours stronger binding with the additive molecules. The lesser hydration of CTAB micelles as compared to those of DTAB and TTAB may also be the reason for the stronger binding of probes with CTAB micelles.

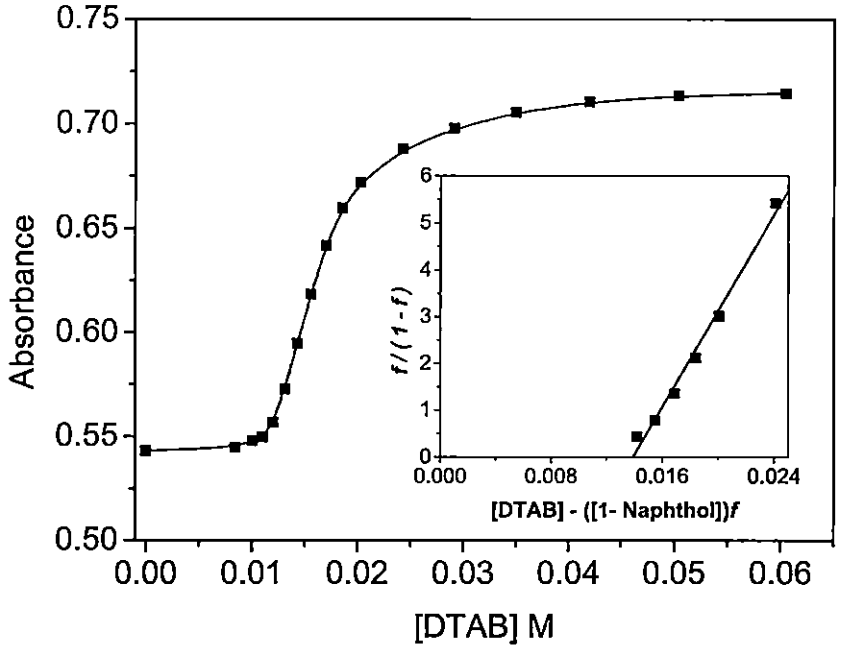

Figure 4.45. Plot of absorbance of 1-naphthol (0.25 mM) against the concentration of aqueous DTAB. The value of K_s (binding constant) were determined from the slope of the plot in the inset.

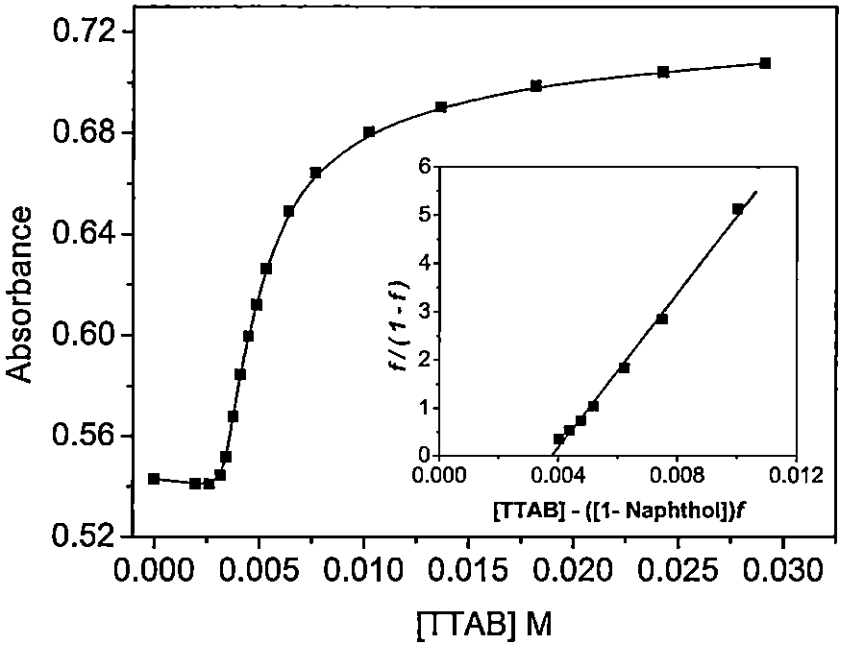

Figure 4.46. Plot of absorbance of 1-naphthol (0.25 mM) against the concentration of aqueous TTAB. The value of K_s (binding constant) were determined from the slope of the plot in the inset.

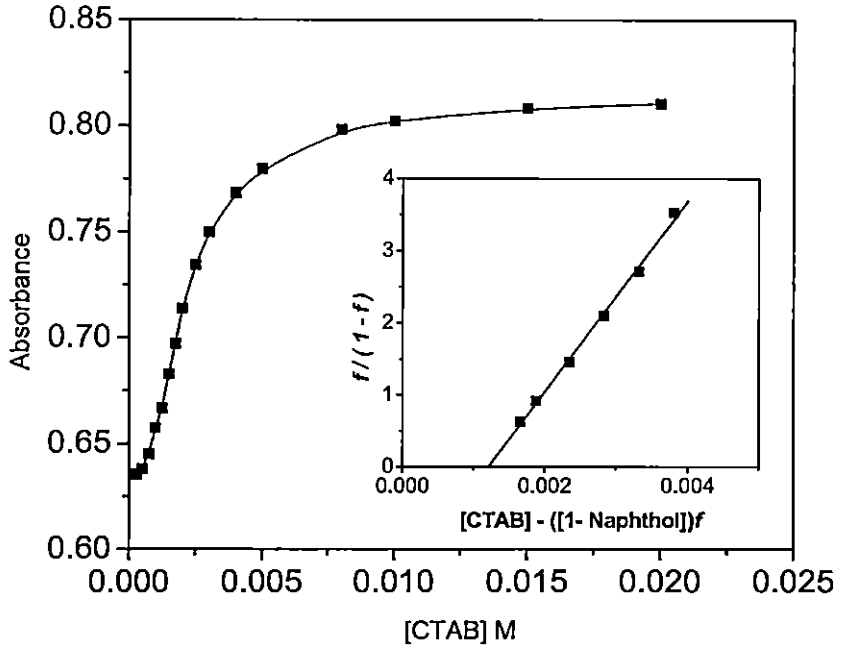

Figure 4.47. Plot of absorbance of 1-naphthol (0.25 mM) against the concentration of aqueous CTAB. The value of K_s (binding constant) were determined from the slope of the plot in the inset.

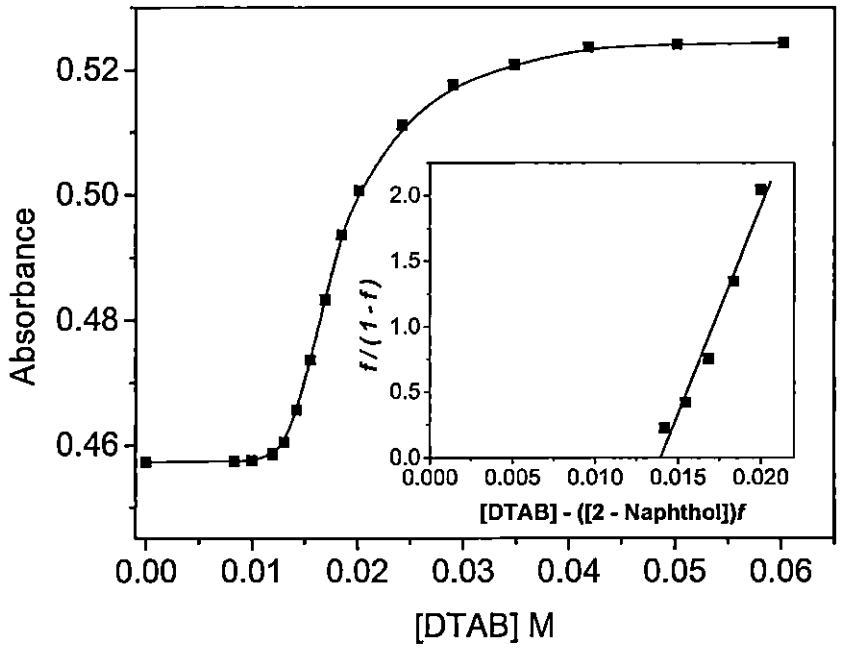

Figure 4.48. Plot of absorbance of 2-naphthol (0.25 mM) against the concentration of aqueous DTAB. The value of K_s (binding constant) were determined from the slope of the plot in the inset.

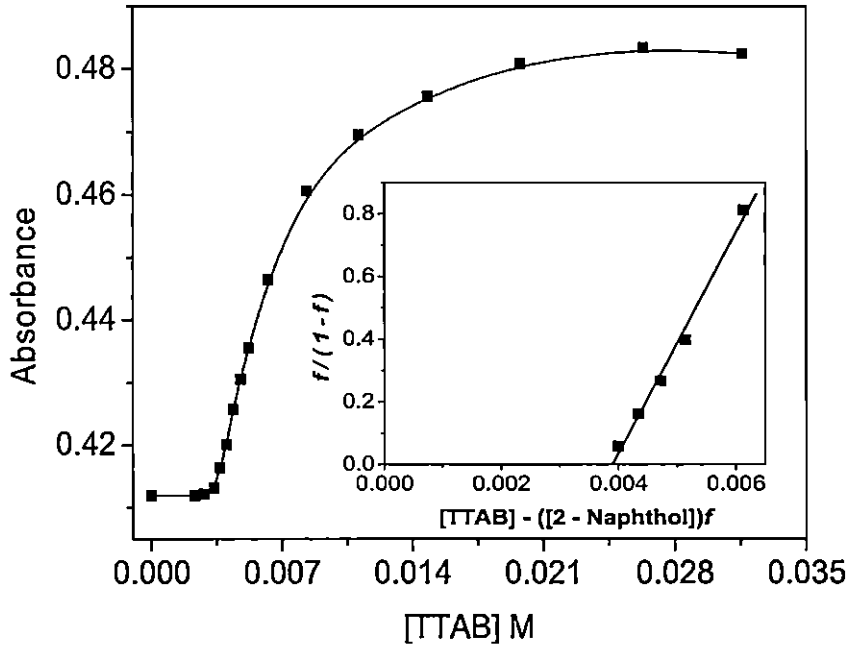

Figure 4.49. Plot of absorbance of 2-naphthol (0.25 mM) against the concentration of aqueous TTAB. The value of K_s (binding constant) were determined from the slope of the plot in the inset.

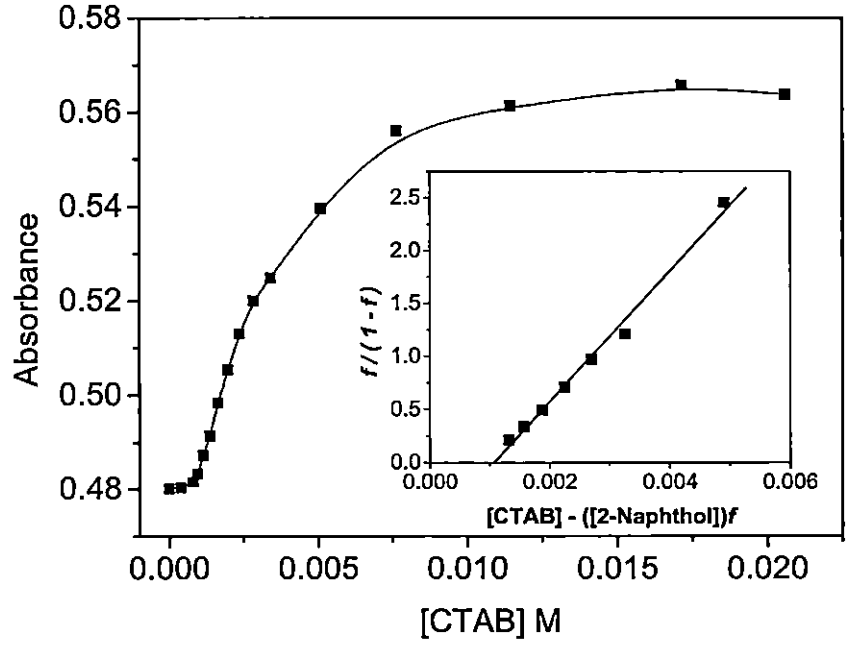

Figure 4.50. Plot of absorbance of 2-naphthol (0.25 mM) against the concentration of aqueous CTAB. The value of K_s (binding constant) were determined from the slope of the plot in the inset.

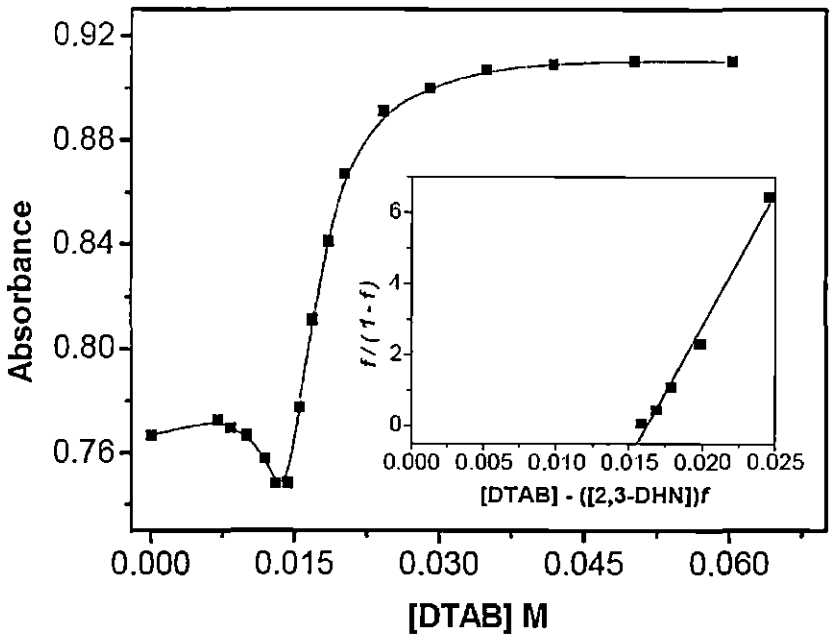

Figure 4.51. Plot of absorbance of 2,3-dihydroxynaphthalene (0.25 mM) against the concentration of aqueous DTAB. The value of K_s (binding constant) were determined from the slope of the plot in the inset.

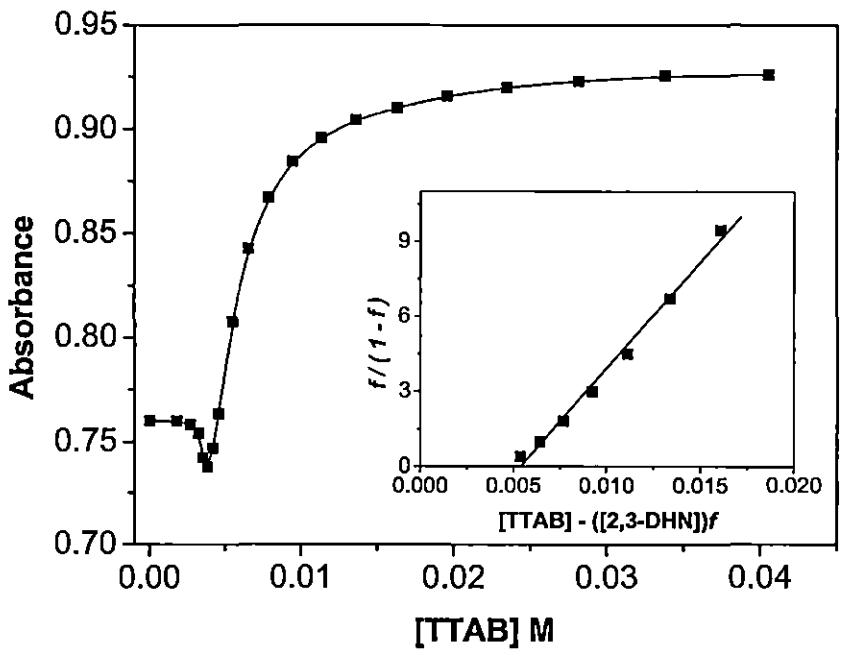

Figure 4.52. Plot of absorbance of 2,3-dihydroxynaphthalene (0.25 mM) against the concen-tration of aqueous TTAB. The value of K_s (binding constant) were determined from the slope of the plot in the inset.

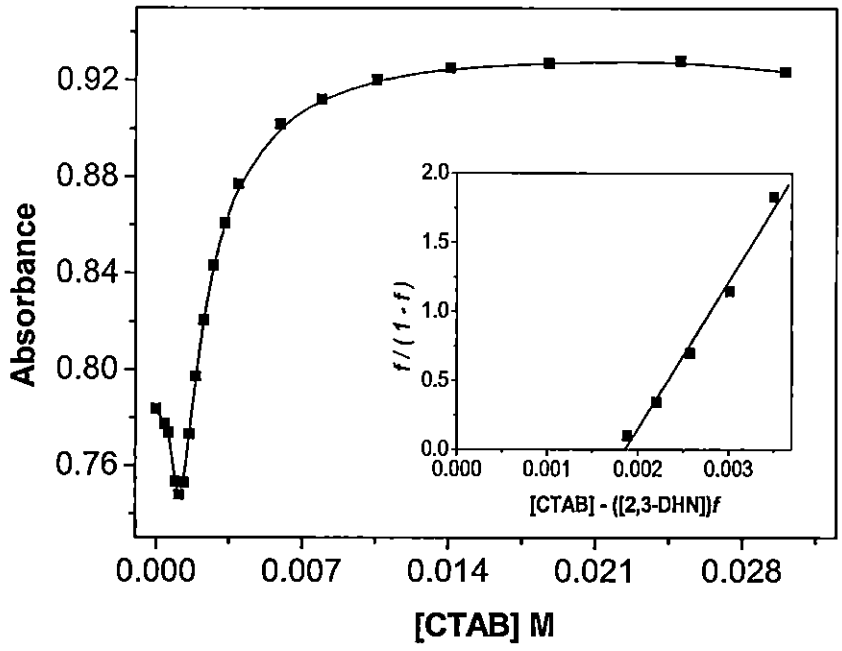

Figure 4.53. Plot of absorbance of 2,3-dihydroxynaphthalene (0.25 mM) against the concen-tration of aqueous CTAB. The value of K_s (binding constant) were determined from the slope of the plot in the inset.

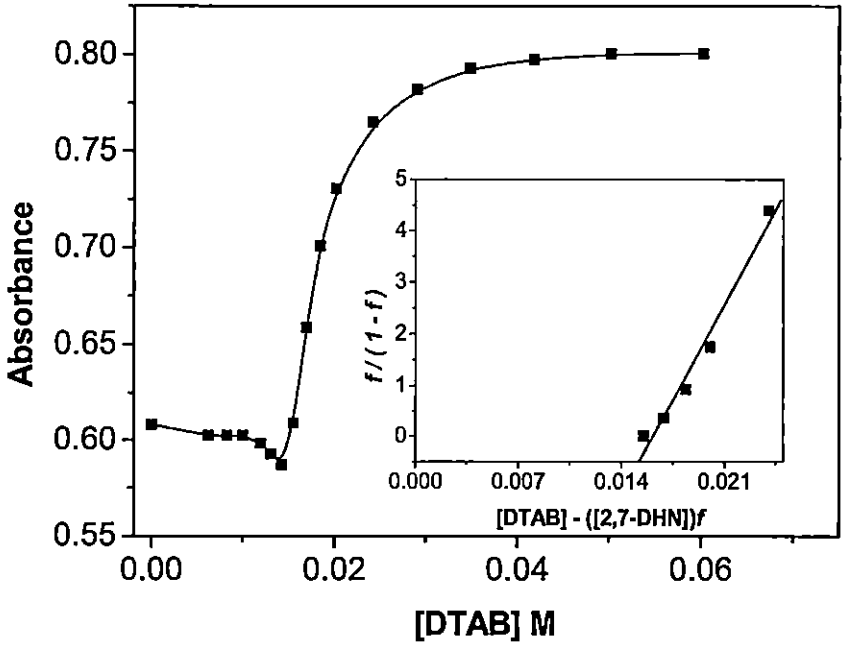

Figure 4.54. Plot of absorbance of 2,7-dihydroxynaphthalene (0.25 mM) against the concentration of aqueous DTAB. The value of K_s (binding constant) were determined from the slope of the plot in the inset.

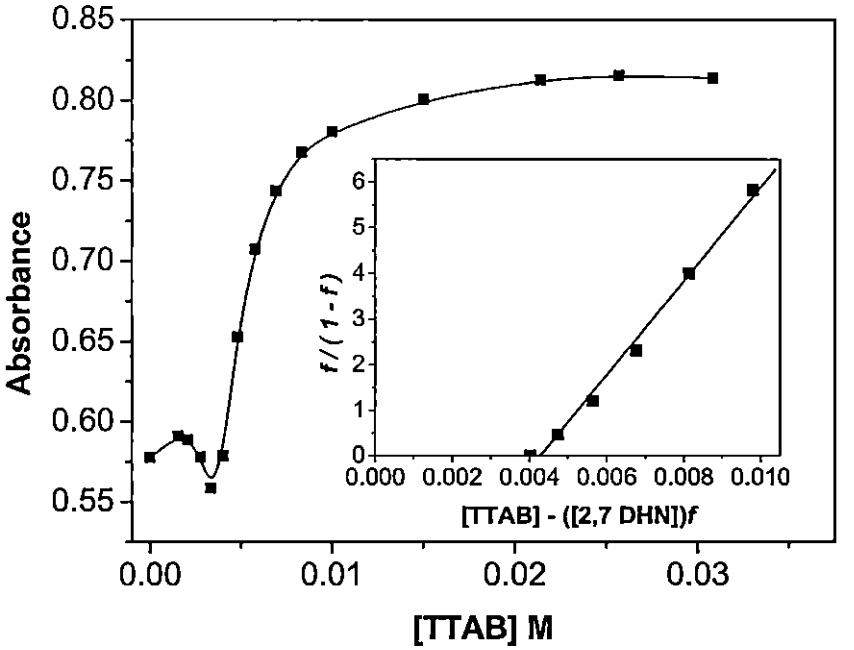

Figure 4.55. Plot of absorbance of 2,7-dihydroxynaphthalene (0.25 mM) against the concen-tration of aqueous TTAB. The value of K_s (binding constant) were determined from the slope of the plot in the inset.

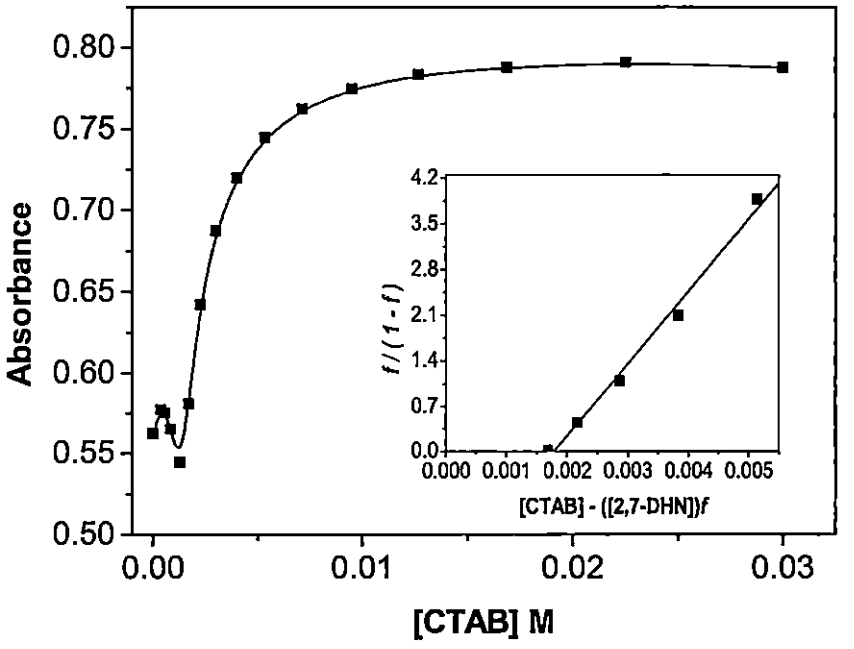

Figure 4.56. Plot of absorbance of 2,7-dihydroxynaphthalene (0.25 mM) against the concen-tration of aqueous CTAB. The value of K_s (binding constant) were determined from the slope of the plot in the inset.

Table 4.1. Values of the binding constants and the cmc determined from the UV absorption studies.

Dopant	Surfactant	K_s	r	cmc $x10^3$ mM
	DTAB	514	0.9942	14.7
1-Naphthol	TTAB	801	0.9989	3.3
	CTAB	1325	0.9981	1.0
	DTAB	505	0.9840	14.5
2-Naphthol	TTAB	638	0.9918	3.2
	CTAB	723	0.9953	1.1
	DTAB	745	0.9925	14.7
2,3-DHN	TTAB	768	0.9974	3.4
	CTAB	1061	0.9845	1.1
	DTAB	529	0.9916	14.8
2,7-DHN	TTAB	1029	0.9964	3.4
	CTAB	1110	0.9896	1.1
1-MN	CTAB	448	0.9918	-
2-MN	CTAB	326	0.9848	-

Therefore, greater the compactness of the microstructure stronger is the binding between the probe and the micelle and vice-versa. Though the binding constant values of the surfactants follow the above order, no systematic trend was observed for the different probes in micellar media.

4.3.6. Cryogenic Transmission Electron Microscopy (cryo-TEM) Study.

Cryo-TEM images of the CTAB-2-naphthol system at low and high pH's are shown in Figures 4.57 to 4.59. At low pH (pH ~5.5), the micrograph looks like a condense, isotropic, and continuous network (Figure 4.57) of worm-like micelles along with monodisperesed vesicles of very short diameters.

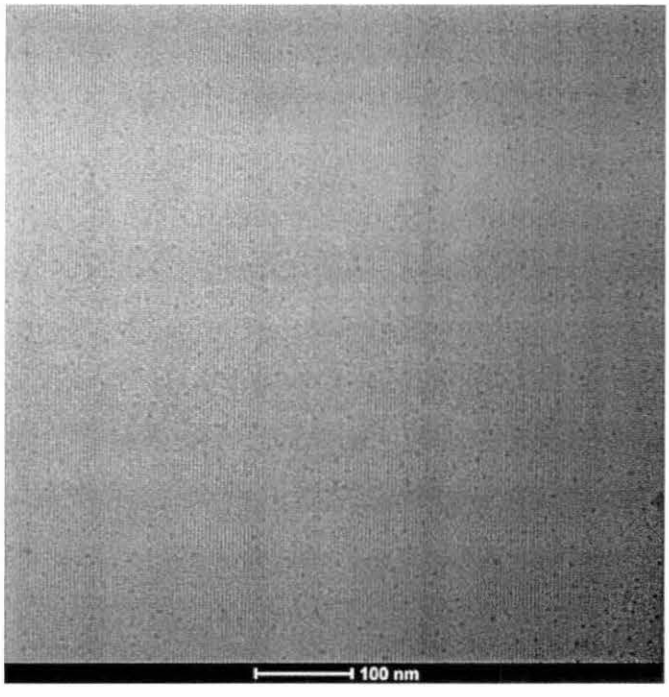

Figure 4.57. cryo-TEM micrographs of the CTAB-2-naphthol system (10 mM, 1:1) at pH ~5.5.

The micelles are slightly entangled and are shown in figure 4.58. At high pH (pH~9.4), the system contains very long (endless in micrograph) wormlike micelles, which coexist with large unilamellar vesicles. This is undoubtedly due to

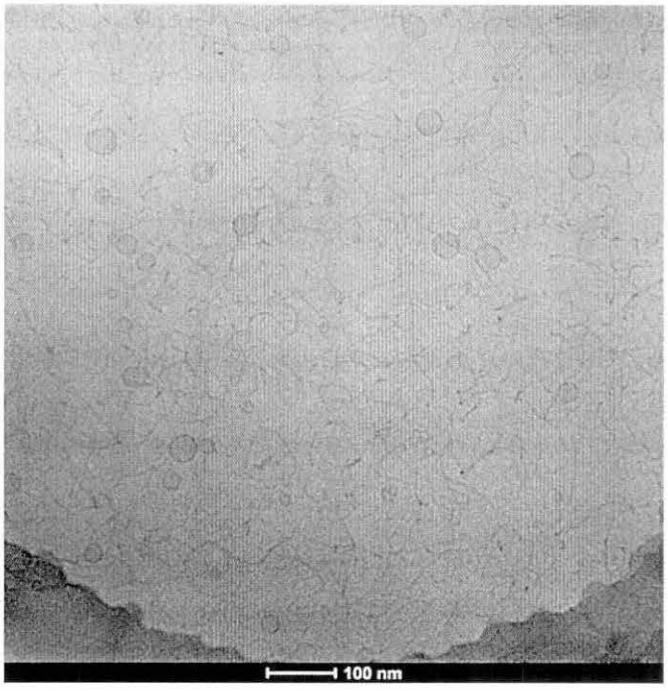

Figure 4.58. cryo-TEM micrographs of the CTAB-2-naphthol system (10 mM, 1:1) at pH of ~9.4)

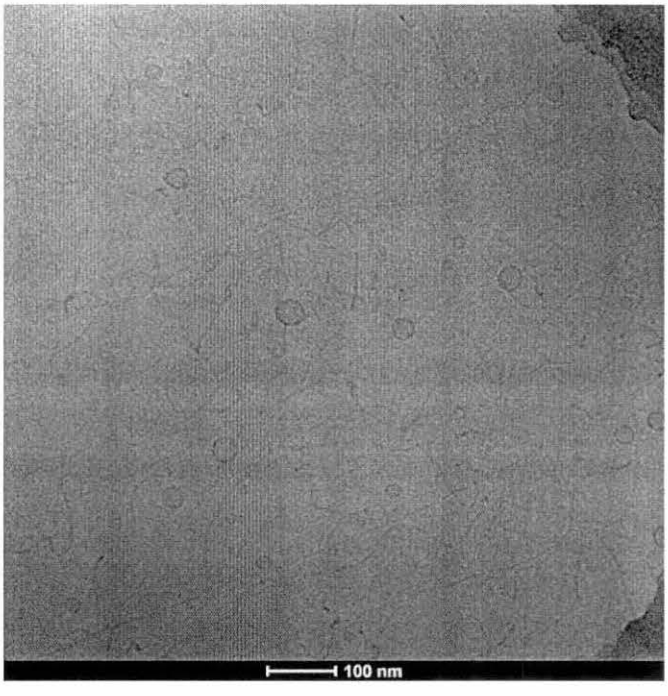

Figure 4.59. cryo-TEM micrographs showing linearly elongated worm-like micelles of the CTAB-2-naphthol system (10 mM, 1:1) at high pH (~9.4) under shear flow.

enhanced charge screening of micelles by naphtholate anions (discussed in section 4.3.3). The field is seen to populate mainly by large vesicles of diameter ~30 nm along with thinly populated smaller vesicles. It is also seen that the long worm-like micelles are highly entangled. Sometimes they are found to elongate linearly under shear flow (Figure 4.59). The solutions are completely transparent. The direct imaging by cryo-TEM supports the rheological observation as a function of pH. At low pH, the worm-like micelles are formed via headgroup charge shielding by aromatic π electrons, whereas, at high pH, ionization of OH groups takes place and the packing parameter exceeds the critical value of 1/2 via enhanced charge screening by naphtholate ions. This leads to unilamellar vesicle formation along with long worm-like micelles.

4.3.7. Orientation of water molecules at the micelle-water interface

Phospholipid bilayers, the main constituent of cell membranes, are important structural components in biological systems. The membrane/water interface provides a unique environment for many biochemical reactions, and the associated interfacial water is an integral part of such reactions. Water in this restrictive environment behaves differently, which affects many biochemical reactions. Therefore, a molecular level elucidation of the structure and orientation of water and lipid/water interfaces is essentially important to understand the adsorption and desorption of various biomolecules, ions and drugs at the biological interfaces [77-80]. In spite of its importance, we are yet to have a unanimous understanding of the water structure even for very simple lipid/water interfaces.

Recently vibrational sum frequency generation (VSFG) study, which is an interface specific spectroscopy, on charged lipid/water interfaces, confirms that the orientation of interfacial water is governed by the net charge on the lipid head group [78-80]. At an anionic lipid/water interface, water is in the hydrogen up orientation, and at the cationic lipid/water interface, water is in the hydrogen down orientation. At the cationic and anionic lipid/water interface, interfacial water has comparable hydrogen bond strength, and it was analogous to the bulk water. In this section of the thesis spectroscopic results are revisited to confirm the

orientation and restructuring of water molecules at the cationic micelle-water interface and demonstrated that H-bonding and cationic- π interactions are involved in the formation of viscoelastic gels.

Micelles of different cationic surfactants viz., CTAB, OTAB, CPB, CPC etc., behave similarly in the presence of π-conjugated molecules with hydrogen bonding functionality like 1-naphthol, 2-naphthol, dihydroxynaphthalenes and alkyl substituted phenols [57, 81-84]. These systems form stimuli responsive viscoelastic gels at low surfactant concentrations. Role of aromatic π-electron systems in screening the charge of cationic head groups in spherical micelles is obvious. Interestingly, another aromatic π-electron system viz., methoxynaphthalenes failed to tune viscoelastic gelation in the above cationic surfactant system. In section 4.2.2 of the thesis it has been shown that the UV absorption spectra of micelle embedded naphthols provides some interesting results. The spectroscopic data strongly indicates the formation of unusual H-bond at the micellar interface by the dopant molecules with interfacial water. It has been argued that the OH groups of naphthols can act as both a proton donar as well as proton acceptor in forming intermolecular H-bonds. H-bond in which the hydroxyl groups of naphthols is proton donor releases electron density from the O-H bond towards the oxygen and hence, by an inductive effect, toward the aromatic ring. This causes red shift of the π- π^* transition. Conversely, if the H-bond is formed in which the hydroxyl oxygen is a proton acceptor, electrons are withdrawn from the naphthalene ring, and an opposite shift is anticipated. In the present case, a significant red shift starts to occur (6.4 nm at λ_{max} ~293 nm) in the presence of CTAB just above its cmc (0.96 mM) with an well defined isobestic point at 296 nm. Such shifting of the λ_{max} continue to occur until most of the naphthols are partitioned in CTAB micelles at high surfactant concentration. The results suggest that the protruded OH groups of micelle-embedded naphthols form H-bond with interfacially located water molecules and acts as hydrogen donars. The spectral characterstics and the nature and the degree of shift resemble the spectra of naphthols in isooctane at various dioxane concentrations, where naphthols acts as H-donar and dioxane as the acceptor (figure 4.26). Previously, it has been shown that in the ground state 1-naphthol interacts with bulk water via

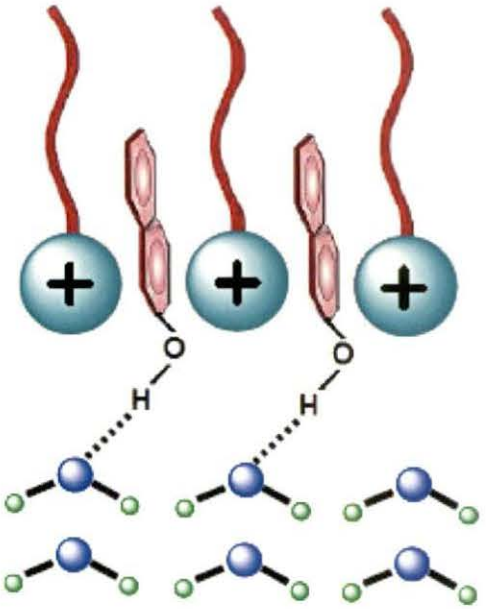

Figure 4.60. Schematic representation of the orientation of water molecules at the micelle water interface.

oxygen [66]. The nature of spectral modifications encountered by micelle free naphthol molecules in the presence of water is shown in figure 4.27. The figure shows that on every addition of water (upto 10 % v/v) substantial gain in intensity is displayed by 1-naphthol spectra with little change in wavelength. The result of the study confirms the orientation of water molecules at the micelle/water interface (figure 4.60) i.e., the electrostatic potential of the positive charges of surfactant head groups orient the water dipoles in hydrogen down direction such that the protruded OH groups can only form H-bonds with oxygen atoms of water as the acceptor site. In such a situation both the hydrogen atoms of water are directed away from the micellar head groups restricting the possibility of formation of H-bonds where water hydrogens might be donar. This result is in perfect agreement with the recent observation found via VSFG studies.

References

1. Fuhrop, J. H.; Köning, J. *Membranes and Molecular Assemblies: the Synkietic Approach*; The Royal Society of Chemistry: Cambridge, 1994.
2. Clint, J. H. *Surfactant Aggregation;* Blackie: Glasgow/London, 1992.
3. Rosen, M. J. *Surfactants and Interfacial Phenomena,* Wiley-Interscience: New York, 2004.
4. Reiss-Husson, F.; Luzzati, V. *J. Phys. Chem.* **1964**, 68, 3504.
5. Ekwall, P.; Mandell, L.; Solyom, P. *J. Colloid Interface Sci.* **1971**, 35, 519.
6. Fontell, K.; Khan, A.; Lindström, B.; Maciejewska, D.; Puang-Ngern, S. *Colloid Polym. Sci.* **1991**, 269, 727.
7. Porte, G.; Poggi, Y.; Appell, J.; Maret, G. *J. Phys. Chem.* **1984**, 88, 5713.
8. Debye, P.; Anacker, E.W. *J. Phys. Chem.* **1950**, 55, 644.
9. Quirion, F.; Magid, L.J. *J. Phys. Chem.* **1986**, 90, 5435.
10. Candau, S.J.; Hirsch, E.; Zana, R. *J. Colloid Interface Sci.* **1985**, 105, 521.
11. Missel, P.J.; Mazer, N.A.; Benedeck, G.B.; Carrey, M.C. *J. Phys. Chem.* **1983**, 87, 1264.
12. Magid, L.J.; Li, Z.; Butler, P.D.; *Langmuir.* **2000**, 16, 10028.
13. Mu, J. H.; Li, G. Z.; Jia, X. L.; Wang, H. X.; Zhang, G.Y. *J. Phys. Chem. B.* **2002**, 106, 11685.
14. Mu, J. H.; Li, G. Z.; Wang, H. X. *Rheol. Acta.* **2002**, 41, 493.
15. Yu, L.J.; Saupe, A. *Phys. Rev. Lett.* **1980**, 45, 1000.
16. Hendrikx, Y.; Charvolin, J.; Rawiso, M.; Liébert, L.; Holmes, M.C. *J. Phys. Chem.* **1983**, 87, 3991.
17. Amaral, L.Q.; Helene, M.E.M. *J. Phys. Chem.* **1988**, 92, 6094.
18. Thiele, T.; Berret, J.F.; Muller, S.; Schmidt, C. *J. Rheol.* **2001**, 45, 29.
19. Porte, G.; Gomati, R.; Haitamy, O.E.; Appell, J.; Marignan, J. *J. Phys. Chem.* **1986**, 90, 5746.
20. Nastishin, Y.A. *Langmuir.* **1996**, 11, 5011.
21. Bijma, K.; Engberts, J.B.F.N. *Langmuir.* **1997**, 13, 4843.
22. Bijma, K.; Bandamer, M.J.; Engberts, J.B.F.N. *Langmuir.* **1998**, 14, 79.
23. Bergström, M.; Pedersen, J.S. *Langmuir.* **1999**, 15, 2250.
24. Yin, H.; Mao, M.; Huang, J.; Fu, H. *Langmuir.* **2002**, 18, 9198.

25. Kaler, E.W.; Herrington, K.L.; Murthy, A.K.; Zasadzinski, J.A.N. *J. Phys. Chem.* **1992**, 96, 6698.

26. Koehler, R.D.; Raghavan, S.R.; Kaler, E.W. *J. Phys. Chem. B.* **2000**, 104, 11035.

27. Nash, T. *J. Colloid Sci.* **1958**, 13, 134.

28. Ulmius, J.; Wennerström, H.; Johansson, L. B. Å.; Lindblom, G.; Gravsholt, S. *J. Phys. Chem.* **1979**, 83, 2232.

29. Gravsholt, S. *J. Colloid Interface Sci.* **1976**, 57, 575.

30. Doi, M.; Edwards, S.F. *The Theory of Polymer Dynamics*, Oxford, Clarendon Press. 1986

31. Rehage, H.; Hoffmann, H. *Mol. Phys.* **1991**, 74, 933.

32. Hoffmann H.; Löbl H.; Rehage H.; Wunderlich I. *Tenside Detergents.* **1985**, 22, 290.

33. Rehage H.; Hoffmann H. *Phys. Chem.* **1988**, 92, 4712.

34. Shikata, T.; Hirata, K.; Kotaka T. *Langmuir.* **1987**, 3, 1081.

35. Shikata, T.; Hirata, K.; Kotaka, T. *Langmuir.* **1988**, 4, 354.

36. Shikata, T.; Hirata, K.; Kotaka, T. *Langmuir.* **1989**, 5, 398.

37. Shikata, T.; Hirata, K.; Kotaka, T. *J. Phys. Chem.* **1990**, 94, 3702.

38. Kern, F.; Zana, R.; Candau, S. J. *Langmuir.* **1991**, 7, 1344.

39. Khatory, A.; Lequeux, F.; Kern F.; Candau, S.J. *Langmuir.* **1993**, 9, 1456.

40. Narayanan, J.; Mendes, E.; Monohar, C. *International Journal of Modern Physics B.* **2002**, 16, 375.

41. Mendes, E.; Oda, R.; Monohar, C.; Narayanan, J. *J. Phys. Chem. B* **1998**, 71, 338.

42. Mishra, S.; Mishra, B. K.; Samant, S. D.; Narayanan, J.; Manohar, C. *Langmuir.* **1993**, 9, 2804.

43. Oda R.; Narayanaa, J.; Hassan, P. A.; Manohar, C.; Salkar, R. A.; Kern, F.; Candau, S.J. *Langmuir* **1998**, 14, 4364.

44. Hassan, P. A.; Candau, S.J.; Kern, F.; Manohar, C. *Langmuir* **1998**, 14, 6025.

45. Lequeux, F. *Europhys. Lett.* **1992**, 19, 675.

46. Mishra, B. K.; Samant, S. D.; Pradhan, P.; Mishra, B.; Manohar, C. *Langmuir* **1993**, 9, 894.

47. Hassan, P. A.; Valaulikar, B. S.; Monhar, C.; Kern, F.; Bourdieu, L.; Candau, S. J. *Langmuir* **1996**, 12, 4350.

48. Kalur, G. C.; Frounfelker, B. D.; Cipriano, B. H.; Norman, A. I.; Raghavan. S. R. *Langmuir* **2005**, *21*, 10998.

49. Israclachivli, J. N.; Mitchell D. J.; Ninham, B. W. *J. Chem. Soc.Faraday Trans.* **1976**, *72*, 1525.

50. Rao, U. R. K.; Manohar, C.; Valaulikar, B. S.; Iyer, R. M. *J. Phys.Chem.* **1987**, *91*, 3286.

51. Takemura, T.; Hara, K.; Baba, H. *Bull. Chem. Soc. Jpn.* **1971**, 44, 977.

52. Hara, K.; Baba, H. *Mol. Phys.* **1974**, 18, 1100.

53. Mataga, N.; Kaifu, Y. J. *Chem. Phys.* **1962**, 36, 2804.

54. Baba, H.; Suzuki, S. *J. Chem. Phys.* **1961**, 35, 1118.

55. Tramer, A.; Zaborowska, M. *Acta Phys. Pol.* **1968**, 34, 821.

56. Karmakar, R.; Samanta, A. *Chem. Phys. Lett.* **2003**, 376, 638.

57. Saha, S.K.; Jha, M.; Ali, M.; Chakraborty, A.; Bit, G.; Das., S.K. *J. Phys. Chem. B.* **2008**, 112, 4642

58. Dougherty, D. A. *Science* **1996**, *271*, 163.

59. Harwigsson, I.; Hellsten M. *J. Am Oil Chem Soc* **1996**, 73, 921.

60. Myska, J.; Chara, Z. *Exp Fluids* **2001**, 30, 229.

61. Lin, Y.; Han, X.; Huang, J.; Fu, H.; Yu, C. J. *Colloid Interface Sci.* **2009**, *330*, 449.

62. Tata, M.; John, V. T.; Waguespack, Y. Y.; McPherson, G. L. *J. Phys. Chem.* **1994**, 98, 3809.

63. Grieser, F., Drummond, C. J. *J. Phys. Chem.* **1988**, 92, 5580.

64. Das, S. K. *Ph.D. Thesis*, University of North Bengal, India, 2006

65. Nemethy, G.; Ray, A. *J. Phys. Chem.* **1973**, *77*, 64.

66. Zharkova, O. M.; Korolev, B. V.; Morozova, Y. P. *Russ. Phys. J.* **2003**, 46, 68.

67. Ramachandran, C.; Pyter, R. A.; Mukherjee, P. *J. Phys. Chem.* **1982**, 86, 3198.

68. Bhattacharya, K. *J. Fluoresc.* **2001**, 11, 167.

69. Balasubramanian, S.; Pal, S.; Bagchi, B. *Curr. Sci.* **2002**, 82, 845.

70. Gasjo, J.; Anderson, E.; Forsbeing, J.; Aziz, E. F.; Brena, B.; Johansson, C.; Nordgren, J.; Duda, L.; Adersson, J.; Hennies, F.; Rubensson, J.; Hansson, P. *J. Phys. Chem. B* **2009**, *113*, 8201.

71. Mallick. A.; Haldar, B.; Maiti, S.; Chattopadhyay, N. *J. Colloid. Interface Sci.* **2004**, 278, 215.

72. Berr, S.; Jones, R. R. M.; Johnson, J. S. *J. Phys. Chem.* **1992**, 96, 5611.

73. Muller, N. In *Reaction Kinetics in Micelles*; Cordes, E. A., Ed.; Plenum Press: New York, 1973

74. Bardez, E.; Monnier, E.; Valeur, B. *J. Colloid Interface Sci.* **1986**, 112, 200.

75. Akbas, H.; Taner, T. *Spectrochim. Acta A.* **2009**, 73, 150.

76. Weidemaier, K.; Tavernier, H.L.; Fayer, M.D. *J. Phys. Chem. B.* **1997**, 101, 9352.

77. Yokota, A.; Tsumoto, K.; Shiroishi, M.; Kondo, H.; Kumagai, I. *J. Biol. Chem.* **2003**, 278, 5410.

78. Mondal, J.A.; Nihonyanagi, S.; Yamaguchi, S.; Tahara, T. *J. Am. Chem. Soc.* **2010**, 132, 10656.

79. Nihonyanagi, S.; Yamaguchi, S.; Tahara, T. *J. Chem. Phys.* **2009**, 130, 204704.

80. Savago, M.; Vartianien, E.; Bonn, H.; *J. Chem. Phys.* **2009**, 131, 161107.

81. Ali, M.; Jha, M.; Das, S. K.; Saha, S. K.; *J. Phys. Chem. B* **2009**, 113, 15563.

82. Singh, M.; Ford, C.; Agarwal, V.; Fritz, G.; Bose, A.; John, V. T.; McPherson, G. L. *Langmuir* **2004**, 20, 9931.

83. Ford, C.; Singh, M.; Lawson, L.; He, J.; John, V.; Lu, Y.; Papadopoulos, K.; McPherson, G.; Bose, A. *Colloids Surf. B.* **2004**, 39, 143.

84. Agarwal, V.; Singh, M.; McPherson, G.; John, V.; Bose, A. *Colloids Sur., A.* **2006**, 281, 246